RHEOLOGICAL FOUNDATIONS OF THE HYDRAULIC TRANSPORT OF CEMENT PASTES

WSPÓŁCZESNE PROBLEMY BUDOWNICTWA

I

Jan Kempiński
Robert Świerzko

RHEOLOGICAL FOUNDATIONS OF THE HYDRAULIC TRANSPORT OF CEMENT PASTES

Wrocław 2010 UWP

Autorzy:
prof. dr hab. inż. Jan Kempiński
mgr inż. Robert Świerzko

Opiniodawca
prof. dr hab. inż. Marek Sozański

Redaktor merytoryczny
dr hab. inż. Krzysztof Pulikowski, prof. nadzw.

Opracowanie redakcyjne
mgr Elżbieta Winiarska-Grabosz

Korekta
mgr Anna Piskor

Łamanie
Teresa Alicja Chmura

Projekt okładki
Halina Sebzda

Monografie CVIII

ISSN 1898–1151
ISBN 978–83–7717–041–0

WYDAWNICTWO UNIWERSYTETU PRZYRODNICZEGO WE WROCŁAWIU
Redaktor Naczelny – prof. dr hab. Andrzej Kotecki
ul. Sopocka 23, 50–344 Wrocław, tel. 71 328–12–77
e-mail: wyd@up.wroc.pl

Nakład 100 + 16 egz. Ark. wyd. 4,0. Ark. druk. 4,75
Druk i oprawa: F.P.H. „ELMA”

SPIS TREŚCI

List of symbols **7**

Introduction **9**

1. Theoretical foundations of rheology of liquid cement pastes **11**

1.1. Rheological models of cement pastes 12
1.2. Actual flow curves 14

2. Study of the rheological properties of cement pastes **17**

2.1. Characteristics of the studied material 17
2.2. Methodology of the tests 18
2.3. Results of rheological tests of cement pastes 20
2.4. Selected rheological model 25
2.5. Analysis of test results 28

3. Boundary parameters of laminar flow during pipe transport **33**

3.1. Marginal concentration 33
3.2. Minimal transient velocity in horizontal pipelines 34
3.3. Laminar flow in the pipe 40
3.4. Determination of the critical Reynolds number Re_{kr} 42
3.5. Determination of the Darcy friction factor 49
3.6. The determination of head loss in horizontal pipelines 59

4. Co-operation of the pumping engine with the pressure pipe **65**

5. Conclusion **69**

Bibliography **71**

List of symbols

Latin alphabet

h_{str} – Head loss [m]
g – Acceleration of gravity [m·s^{-2}]
n – Flow behaviour index [–]
v – Linear velocity [m·s^{-1}]
v_{gr} – Transient velocity [m·s^{-1}]
v_{kr} – Critical velocity [m·s^{-1}]
w – Sedimentation rate [m·s^{-1}]
C_s – Mass concentration [%]
C_V – Volume concentration [%]
D – Pipe diameter [m]
I_m – Decrease of energy line [–]
K – Consistency index [Pa·s^n]
K_{HB} – Consistency index (Herschel–Bulkley model) [Pa·s^n]
K_V – Consistency index (Vočadlo model) [Pa·s^n]
L – Pipe length [m]
Q – Volumetric flow rate [m^3·s^{-1}]
R_1 – Radius of the internal cylinder in viscometer [m]
R_2 – Radius of the external cylinder in viscometer [m]
Re – Reynolds number [–]
Re_B – Generalized Reynolds number (Bingham model) [–]
$Re_{B,kr}$ – Critical Reynolds number (Bingham model) [–]
$Re_{H,gen}$ – Generalized Reynolds number (Herschel–Bulkley model) [–]
$Re_{H,kr}$ – Critical Reynolds number (Herschel–Bulkley model) [–]
V – Volume [m^3]
W/C – Water to cement ratio [–]

Greek alphabet

α – Square of radius ratio in rotational viscometer [–]
$\dot{\gamma}$ – Shear rate [s^{-1}]
$\dot{\gamma}_p$ – Pseudo-shear rate (Newtonian shear rate) [s^{-1}]
η_{pl} – Plastic viscosity (Bingham model) [Pa·s]
η_C – Plastic viscosity (Casson model) [Pa·s]
η_{Cg} – Plastic viscosity (generalized Casson model) [Pa·s]
λ – Darcy friction factor [–]
ρ – Density [$kg \cdot m^{-3}$]
ρ_m – Mixture density [$kg \cdot m^{-3}$]
ρ_s – Solid particle density [$kg \cdot m^{-3}$]
ρ_w – Water density [$kg \cdot m^{-3}$]
ξ – Minor loss coefficient [–]
τ – Shear stress [Pa]
τ_0 – Yield stress [Pa]
τ_{0B} – Yield stress (Bingham model) [Pa]
τ_{0C} – Yield stress (Casson model) [Pa]
τ_{0Cg} – Yield stress (generalized Casson model) [Pa]
τ_{0HB} – Yield stress (Herschel–Bulkley model) [Pa]
τ_{0V} – Yield stress (Vočadlo model) [Pa]
τ_{R1} – Shear stress on the surface of internal cylinder [Pa]
τ_w – Shear stress on the surface of the pipe [Pa]
Δp – Pressure loss on pipe length [Pa]
Ω – Rotational speed of cylinder in rotational viscometer [$rad \cdot s^{-1}$]

INTRODUCTION

The increasing mechanisation of construction works has made hydraulic transport through pipes an inherent element of the transportation of liquid, cement-derived materials (cement pastes, mortars, fresh concrete). This concerns, in particular, technological chains of injection facilities that constitute a method of repairing concrete structures, reinforcement of rock and soil media, mechanic application of plaster or hydraulic serving of construction concrete.

The term "workability" has been successfully used for many years in the field of concrete and mortar technology. It is interpreted as a widely understood susceptibility of the mixture to formation, without the occurrence of stratification. A descriptive definition of "workability" with use of such terms as workable, hardly workable, non-workable – is pointless from the point of view of technological usability. The major progress in the technology of concretes and applied rheology allows us to prove the complex physical nature of workability. Quantitative and qualitative presentation of workability is connected with numerous problems, which causes doubts as to whether workability can be treated as a physical property of the mixture. According to Szwabowski [28], it is impossible to directly measure workability as a physical property of the mixture. The phenomenon of workability is of a rheological nature and therefore should be analysed basing on viscometric tests.

The subject of rheology is the behaviour of materials under strain, including the aspects of temperature and time. The behaviour of a mixture in any process, under certain strains (pump, vibrator), is determined by its rheological properties [29]. Rheological studies on cement pastes are a universal approach that allows the evaluation and analysis of the workability for any given method and for any production and transport conditions.

Thus, the development of hydraulic chains requires not only the knowledge of the physical and chemical parameters of the transported medium, but also, first of all, a rheological description of its behaviour in the flow phase. A comprehensive rheological characteristic is indispensible.

Hydraulic transport of cement pastes, which is the main topic of this publication, takes place at high concentrations, described as mass concentration, volume concentration, or water to cement ratio *W/C*.

Basic parameters of hydraulic transport consist in the determination of:

- the scope of laminar flow in the given pipeline;
- Darcy friction factor of the pipeline λ;
- head loss on the total length of the pipe;
- working point of the pump-pipe system.

The determination of the parameters and relations listed above will eventually enable the optimisation of the design of technological chains for hydraulic transport of liquid cement pastes.

1. THEORETICAL FOUNDATIONS OF RHEOLOGY OF LIQUID CEMENT PASTES

Rheology is a science concerned with the deformation and flow of materials [4, 9]. Cement paste is a mixture of cement and water [12]. Thus, the rheology of cement pastes by definition deals with the description of the deformation and flow of cement and water mixtures. In the aspect of hydraulic transport the area of interest will be the so-called fresh cement pastes, i.e. pastes during the period between the mixing of cement with water, and the beginning of the binding period.

Rheological properties of fresh cement pastes depend on numerous factors. The major factor influencing the rheological parameters of cement and water mixtures is their concentration, usually described with use of the water to cement ratio *W/C* [18, 32]. Another element that has a significant influence on the rheological properties of cement pastes is their granulometric composition, and thus their specific surface area [32]. Other factors that influence the results obtained in rheological measurements include: the time and method of mixing of pastes [33], temperature [18], chemical and mineral composition [11], and even the applied measurement system [21].

The objectives of rheological studies include, among others, the determination of the rheological parameters of the given medium, which are required in order to explicitly describe its behaviour during the flow. To achieve this objective, the relations between the shear stress τ and the shear rate $\dot{\gamma}$ have to be determined for the widest possible range of shear rates within the laminar movement [23].

Rheological properties of fresh cement pastes are usually measured with use of rotational rheometers, or, less often, pipe or capillary rheometers [3, 18, 28]. In cases when rotational viscometers are used, the most often used are apparatuses with measurement systems based on coaxial cylinders [28], although, according to literature, they have to meet certain requirements: the gap between the internal and external cylinder should not be smaller than ten [3, 25, 28], or even fifteen to twenty times [23] the diameter of the particles of the given mixture. The ratio of the radii of the external and internal cylinders should be lower than 1.2 [3, 25] and the ratio of the height of the internal cylinder to its radius should be higher than one [25].

The results of rheometric measurements of non-Newtonian liquids, such as cement pastes, most often obtained in a discrete form, are usually presented as rheograms, i.e. the relations between the shear stress on the wall of the rotating cylinder τ and the shear rate $\dot{\gamma}$. A specimen of the measurement curve is presented in Figure 1.1.

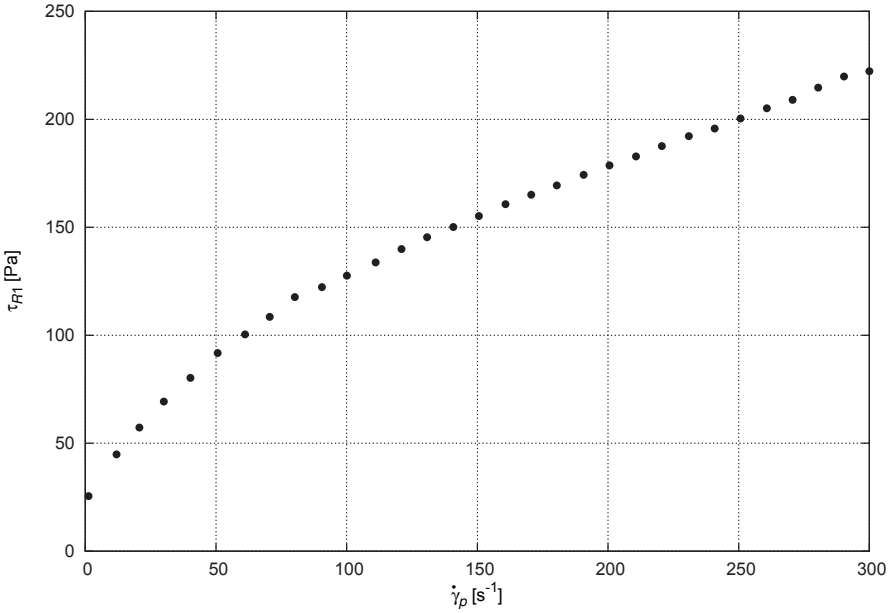

Fig. 1.1. Sample measurement curve obtained during the analysis of cement pastes

1.1. Rheological models of cement pastes

In order to determine the rheological parameters of the analysed mixtures, the rheograms obtained as a result of measurement are then approximated with use of a suitable rheological model. In the case of cement pastes, numerous researchers have suggested a series of rheological models to describe their properties. The basic rheological models used for the description of behaviour of cement pastes are presented below.

Bingham model

$$\begin{aligned} \tau &= \tau_{0B} + \eta_{pl}\dot{\gamma} \quad \text{for} \quad \tau > \tau_{0B} \\ \dot{\gamma} &= 0 \qquad\qquad\quad \text{for} \quad \tau \le \tau_{0B} \end{aligned} \tag{1.1}$$

This is a linear, bi-parametric model, where τ_{0B} is the yield stress, while η_{pl} is the plastic viscosity of the mixture. This model was generally applied for the description of rheological properties of cement pastes [10, 21, 22, 27, 30, 34]. In cases when the yield stress is non-existent ($\tau_0 = 0$) it is simplified to the single-parameter Newton model.

Casson model

$$\begin{aligned} \sqrt{\tau} &= \sqrt{\tau_{0C}} + \sqrt{\eta_C \dot{\gamma}} \quad \text{for} \quad \tau > \tau_{0C} \\ \dot{\gamma} &= 0 \qquad\qquad\qquad\quad \text{for} \quad \tau \le \tau_{0C} \end{aligned} \tag{1.2}$$

This is another bi-parametric model, where τ_{0C} stands for the yield stress, and η_C for the plastic viscosity of the mixture. This model was also often used to describe the rheological properties of cement pastes, although numerous authors pointed to the fact that the results obtained with use of this model were unsatisfactory [2, 21, 22, 34].

Eyring model

$$\tau = a\sinh^{-1}\left(b\dot{\gamma}\right) \tag{1.3}$$

Another bi-parametric rheological model. As opposed to the Bingham and Casson models, it does not take into consideration the yield stress $\tau_{0,}$ and the parameters a and b do not have any corresponding physical equivalents. The model has been successfully applied for the purpose of description of the behaviour of cement pastes in the range of high shear rates [2, 22].

Herschel–Bulkley model

$$\begin{aligned} \tau &= \tau_{0HB} + K_{HB}\dot{\gamma}^n \quad \text{for} \quad \tau > \tau_{0HB} \\ \dot{\gamma} &= 0 \qquad\qquad\qquad\quad \text{for} \quad \tau \le \tau_{0HB} \end{aligned} \tag{1.4}$$

This model belongs to the category of tri-parametric models, where τ_{0HB} is the yield stress, K_{HB} is the consistency index, and n is the flow behaviour index. This model has been successfully used for the description of rheological properties of cement pastes; it offers a good representation of both the occurrence of yield stress, and the curved line of the changes in shear stress as a function of shear rate [2, 6, 21, 22, 34]. The Herschel–Bulkley model can be classified as a general model, because in specific instances it is reduced to simpler, single-parameter and bi-parametric models: for the value of $\tau_0 = 0$ it becomes the Ostwald–De Waele model, for $n = 1$ the Bingham model, and when both of the above conditions appear simultaneously – the Newton model.

Robertson–Stiff model

$$\tau = A\left(\dot{\gamma} + B\right)^C \tag{1.5}$$

This is a general, tri-parametric model, that is reduced to the Ostwald–De Waele model for $B = 0$, Bingham model for $C = 0$ ($\tau_0 = AB$) and to the Newton model in the case when $B = 0$ and $C = 0$ ($\eta = A$). This model was applied with satisfactory results, among others in the cited studies [13, 22, 34].

Vom Berg model

$$\tau = \tau_0 + b\sinh^{-1}\left(\frac{\dot{\gamma}}{c}\right) \tag{1.6}$$

This model is a version of the Eyring model (1.3), with the addition of the yield stress value τ_0. It has been used for the approximation of the flow curves, among others, by the authors of the studies [2, 20, 22, 32], although some of the authors claimed that the results obtained with use of this model are unsatisfactory [2, 22].

Moreover, the authors of this study suggest using, for the purpose of the approximation of measurement data, two models that have not been widely used so far with respect to cement pastes, i.e. the generalized Casson model (1.7) and the Vočadlo model (1.8).

Generalized Casson model

$$\begin{aligned} \tau &= \left[\tau_{0Cg}^{1/n} + \left(\eta_{Cg}\dot{\gamma}\right)^{1/n}\right]^n \quad \text{for} \quad \tau > \tau_{0Cg} \\ \dot{\gamma} &= 0 \qquad\qquad\qquad\qquad\quad \text{for} \quad \tau \le \tau_{0Cg} \end{aligned} \tag{1.7}$$

Vočadlo model

$$\begin{aligned} \tau &= \left(\tau_{0V}^{1/n} + K_V\dot{\gamma}\right)^n \quad \text{for} \quad \tau > \tau_{0Cg} \\ \dot{\gamma} &= 0 \qquad\qquad\qquad\quad \text{for} \quad \tau \le \tau_{0Cg} \end{aligned} \tag{1.8}$$

Both suggested models can be classified as general models, as in specific conditions they are transformed to simpler models, i.e. to the bi-parametric Bingham model ($n = 1$) and the single-parameter Newton model ($n = 1$ i $\tau_0 = 0$).

1.2. Actual flow curves

Fresh cement pastes are liquids of a clearly non-Newtonian nature, due to the occurrence of yield stress and to the curved shape of the changes in stress as a function of shear rate. This means that the flow curves obtained as a result of direct rheological measurements are not actual curves (apparent curves, pseudo-curves) and they should be appropriately adjusted [23].

The pseudo-shear rate ($\dot{\gamma}_p$) and the actual shear rate ($\dot{\gamma}$) are equal only for Newtonian liquids (of constant viscosity, without a yield stress).

For non-Newtonian liquids the actual shear rate depends on the adopted rheological model and on the applied measurement system (the radii of the internal cylinder R_1 and of the external cylinder R_2).

Shear stress in any given point of the interspace of the Couette-Sarle type rotational viscometer, equipped with a measurement system consisting of coaxial cylinders (internal cylinder radius R_1, external cylinder radius R_2), can be described by the following equation:

$$\tau = \frac{M}{2\pi L R^2} \tag{1.9}$$

Where:
τ – shear stress [Pa];
M – torque in relation to the axis of the cylinders [Nm];
L – height of the internal cylinder [m];
R – radius of the cylinder [m]

Thus, the stress on the edge of the rotating internal cylinder of the radius R_1 equals:

$$\tau_{R1} = \frac{M}{2\pi L R_1^2} \tag{1.10}$$

The result of the division of the equations (1.9) and (1.10) gives:

$$\tau = \frac{R_1^2}{R^2}\tau_{R1} = \tau(R) \tag{1.11}$$

Shear rate can be presented as gradient of linear velocity (v) on the width of the interspace of the viscometer. Thus, for $R \in (R_1; R_2)$:

$$\dot{\gamma} = -\frac{\mathrm{d}v}{\mathrm{d}R} = \dot{\gamma}(\tau) \tag{1.12}$$

The relations between the angular velocity (ω) and linear velocity (v) is described by the equation:

$$\omega = \frac{v}{R} \tag{1.13}$$

The differentiation of the equation (1.13) gives:

$$\frac{\mathrm{d}\omega}{\mathrm{d}R} = -\frac{1}{R}\frac{\mathrm{d}v}{\mathrm{d}R} \tag{1.14}$$

And, including the equations (1.12) and (1.11):

$$\mathrm{d}\omega = -\frac{1}{R}\frac{\mathrm{d}v}{\mathrm{d}R} = -\frac{1}{R}\dot{\gamma}\left(\tau(R)\right)\mathrm{d}R \tag{1.15}$$

For rotational Couette-Sarle type viscometer with a rotating internal cylinder, boundary conditions can be expressed as follows:

$$\begin{aligned} \omega &= \Omega \quad \text{for} \quad R = R_1 \\ \omega &= 0 \quad \text{for} \quad R = R_2 \end{aligned} \tag{1.16}$$

Using the above boundary conditions (1.16), basing on the relation (1.15) results in an equation describing the rotational velocity of the rotating internal cylinder:

$$\Omega = \int_{R_1}^{R_2} \frac{1}{R} \dot{\gamma}\left(\tau\left(R\right)\right) \mathrm{d}R \tag{1.17}$$

The solution of the equation (1.17) allows the determination of the actual shear rate of a mixture characterised by a known rheological model.

Literature offers a series of solutions to the problem of the conversion of apparent curves of flow into actual curves of flow and suggest graphical, grapho-analytical [5, 23], analytical [15], and numerical methods [1, 5, 14].

In this study, in order to transform the measured apparent curves of flow into actual curves, the shear rate was adjusted with use of the Krieger, Maron and Elrod equation (1.18), in compliance with the methodology suggested by Czaban [5].

$$\dot{\gamma} = \dot{\gamma}_p \left\{ 1 + K_1 \left(m - 1\right) + K_2 \left[\left(m-1\right)^2 + 0.4343 \frac{\mathrm{d}m}{\mathrm{d}\log\tau_{R1}} \right] \right\} \tag{1.18}$$

Where:

$$K_1 = \frac{\alpha - 1}{2\alpha} \left(1 + \frac{\ln\alpha}{3} \right) \tag{1.19}$$

$$K_2 = \frac{\alpha - 1}{12\alpha} \ln\alpha \tag{1.20}$$

$$\alpha = \frac{R_2^2}{R_1^2} \tag{1.21}$$

and m is the directional coefficient of the tangent in a given point of the curve $\log \dot{\gamma}_p = f(\log \tau_{R1})$

$$m = \frac{\mathrm{d}\log\dot{\gamma}_p}{\mathrm{d}\log\tau_{R1}} \tag{1.22}$$

2. STUDY OF THE RHEOLOGICAL PROPERTIES OF CEMENT PASTES

The evaluation of rheological properties of cement pastes requires not only to conduct viscometric tests, but also to determine the basic physical characteristics of the given medium and the methodology of measurement, which will eventually enable the precise determination of the valid scope of interpretation of the obtained test results.

2.1. Characteristics of the studied material

Rheological tests of cement pastes were conducted with use of mixed Portland cements CEM II/B-S 32.5 R i CEM II/B-S 42.5 N. These cements are a mix of Portland clinker (approx. 65%), granulated furnace slag (approx. 30%) and binding time regulator (gypsum, in the amount of approx. 5%).

The basic physical and chemical properties of the tested cements are presented in Table 2.1.

Table 2.1

Basic properties of the tested cements

Property	CEM II/B-S 32.5 R	CEM II/B-S 42.5 N
Compression strength		
After 2 days [MPa]	17.0	20.1
After 28 days [MPa]	50.8	56.8
Specific amount of water [%]	24.6	29.5
Binding start time [min]	125	180
Binding end time [min]	215	240
Le Chatelier volume change [mm]	2.0	0.8
Specific surface area [$cm^2 \cdot g^{-1}$]	3860	4230
Specific density [$g \cdot cm^{-3}$]	3.072	3.050
Content of SO_3 [%]	2.0	2.1
Content of Cl^- [%]	0.07	0.07

With use of both types of cement and distilled water, cement pastes were prepared, with the water to cement ratio *W/C* varying within the range from 0.35 to 0.70 for cement CEM II/B-S 32.5 R and from 0.40 to 0.70 for cement CEM II/B-S 42.5 N. Mass concentrations C_s and volume concentrations C_V of the tested cement pastes for the respective values of the water to cement ratio *W/C* are presented in Table 2.2. For similar values of specific density, calculated concentration values presented in Table 2.2 were adopted as valid for both types of materials.

Table 2.2

Water to cement ratios, mass concentrations and volume concentrations of the tested cement pastes

Water to cement ratio *W/C*	Mass concentration C_s [%]	Volume concentration C_V [%]
0.35	74.1	48.0
0.40	71.4	44.6
0.50	66.7	39.2
0.60	62.5	35.0
0.70	58.8	31.6

2.2. Methodology of the tests

Rheological tests were conducted with use of the rotational Couette-Sarle viscometer Haake Viscotester VT550, applying the measurement system MV 2 characterised by the following parameters:

- radius of internal cylinder R_1 = 18.4 mm;
- radius of external cylinder R_2 = 21.0 mm;
- height of the internal cylinder L = 60.0 mm;
- width of the measurement interspace 2.6 mm;
- radii quotient R_2/R_1 = 1.14;
- volume of the tested sample V = 46.0 cm^3;
- highest measured shear stress τ_{max} = 230 Pa;
- highest measured shear rate $\dot{\gamma}_{max}$ = 720 s^{-1}.

The rheological testing unit and major measurement systems are presented in Figure 2.1.

Cement pastes were mixed manually, as described below:

- directly after the blending of components they were mixed manually for 90 s;
- the paste was left to rest for 450 s;
- followed by intensive manual mixing for 60 s.

Cement paste prepared in the above described way was then put into the cylinder of the rotational viscometer (MV, Fig. 2.1) where rheological measurements were conducted.

Fig. 2.1. Viscometer Haake VT550 and basic measurement systems

In order to destroy the emerging paste structure [18, 21, 24, 33] prior to the rheological tests the following system of preshearing of the mixture was applied:

- preshearing at the rate of 100 s^{-1} for 60 s;
- preshearing at the rate of 300 s^{-1} for 60 s;
- rest for 10 s;
- preshearing at the rate increasing from 0 to 300 s^{-1} for 60 s.

Directly after the initial shearing cycle, apparent curves of flow were measured at shearing rate decreasing from 300 to 0 s^{-1} during 60 s.
The full measurement cycle, lasting for 250 s, is presented in Figure 2.2.
The tests were conducted at temperature $T = 20^{o}C$.

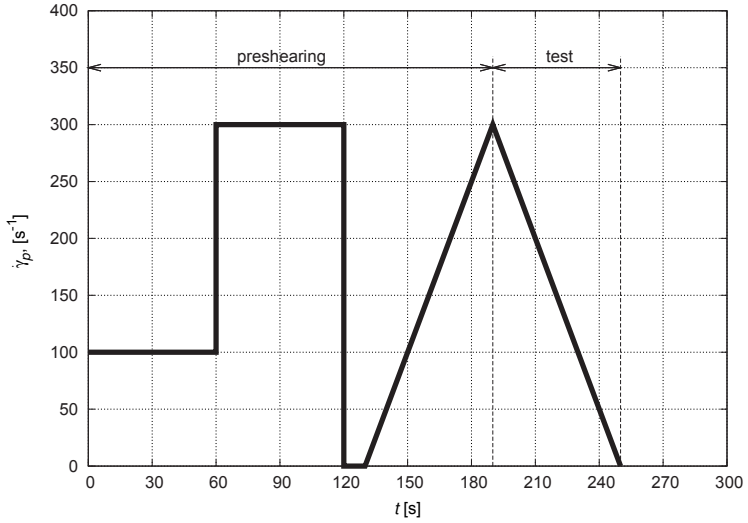

Fig. 2.2. Measurement cycle used for the tests of rheological properties of cement pastes

2.3. Results of rheological tests of cement pastes

As a result of the rheological tests the following apparent curves of flow (pseudo-curves) were obtained, as presented collectively in Figures 2.3 and 2.4.

The apparent curves of flow were approximated with use of the following rheological models:

- Bingham (1.1);
- Casson (1.2);
- Herschel–Bulkley (1.4);
- generalized Casson (1.7);
- Vočadlo (1.8).

In order to transform the measured apparent curves of flow into actual curves, shear rate was adjusted with use of the Krieger, Maron and Elrod equation with Sveč correction (1.18), in compliance with the methodology suggested by Czaban [5].

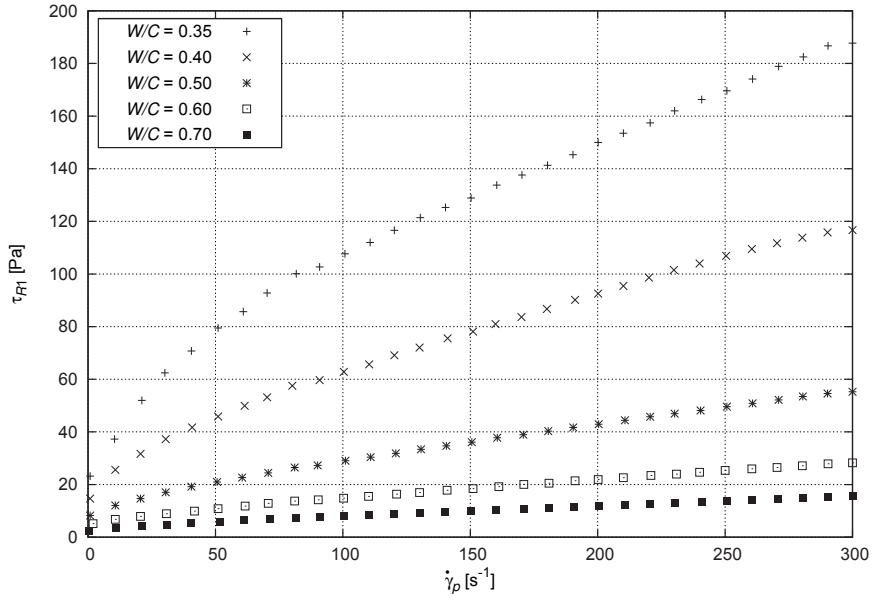

Fig. 2.3. Apparent curves of flow of cement pastes made from cement CEM II/B-S 32.5 R

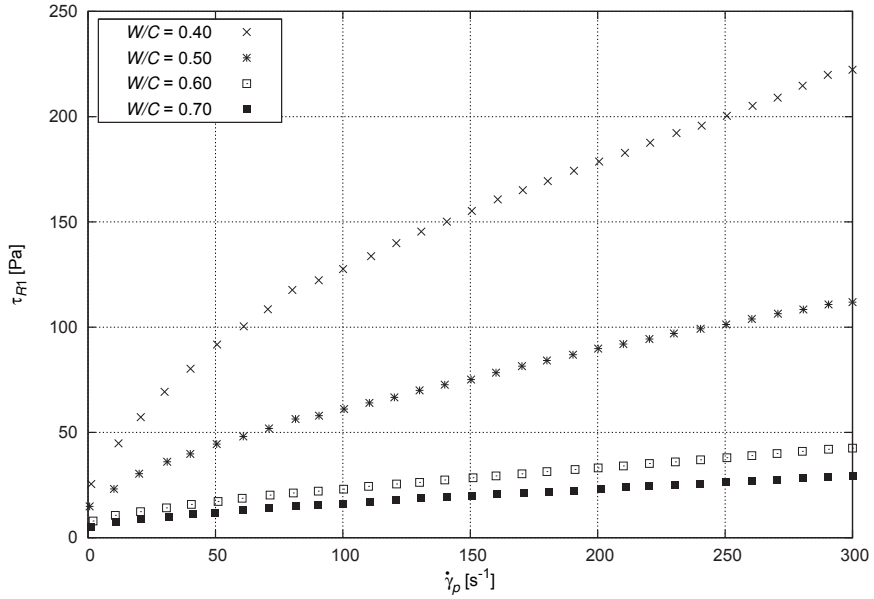

Fig. 2.4. Apparent curves of flow of cement pastes made from cement CEM II/B-S 42.5 n

The obtained actual curves of flow (Fig. 2.5, Fig. 2.6), were approximated, similarly to the case of apparent curves, with use of rheological models 1.1 – 1.8. The results of these calculations are presented in Table 2.3 and Table 2.4.

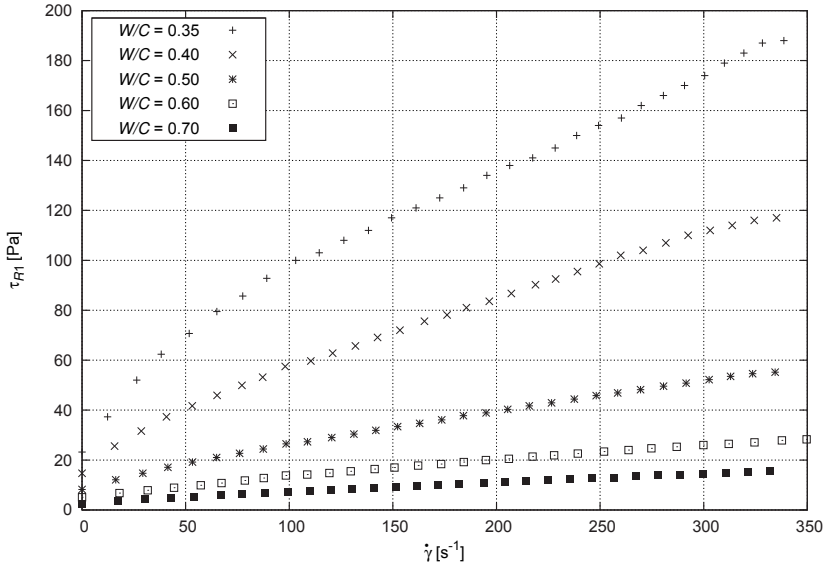

Fig. 2.5. Actual curves of flow of cement pastes made from cement CEM II/B-S 32.5 R

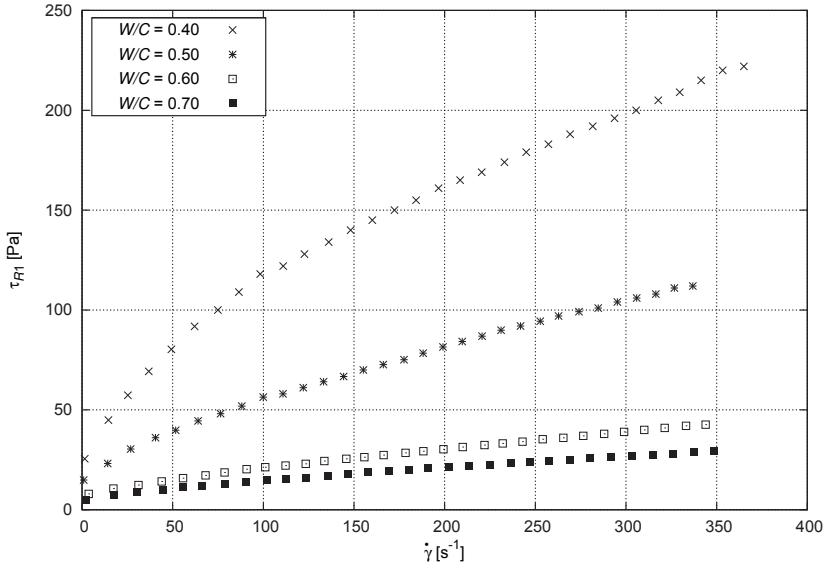

Fig. 2.6. Actual curves of flow of cement pastes made from cement CEM II/B-S 42.5 N

Table 2.3

Rheological parameters of apparent and actual curves of flow of cement pastes made from cement CEM II/B-S 32.5 R, detemined basing on various rheological models

Parameters of apparent curves of flow															
			Bingham		Casson		generalized Casson			Herschel–Bulkley			Vočadlo		
W/C	C_s	C_V	τ_{0B}	η_{pl}	τ_{0C}	η_C	τ_{0Cg}	η_{Cg}	n	τ_{0HB}	K_{HB}	n	τ_{0V}	K_V	n
	[%]	[%]	[Pa]	[Pa·s]	[Pa]	[Pa·s]	[Pa·s]	[Pa]	[–]	[Pa]	[Pa·s^n]	[–]	[Pa]	[Pa·s^n]	[–]
0.35	74.1	48.0	50.3	0.4900	28.0	0.2420	19.3	0.1519	2.6217	21.2	5.1376	0.6095	23.3	72.3881	0.5225
0.40	71.4	44.6	28.2	0.3158	14.8	0.1667	14.0	0.1588	2.0728	15.6	1.8877	0.7004	17.3	7.8185	0.6109
0.50	66.7	39.2	12.9	0.1478	6.7	0.0789	7.9	0.0923	1.7586	8.5	0.6304	0.7559	9.2	1.3171	0.6633
0.60	62.5	35.0	7.0	0.0739	3.7	0.0382	4.9	0.0517	1.5539	5.2	0.2489	0.7943	5.5	0.3716	0.6942
0.70	58.8	31.6	3.6	0.0413	1.8	0.0222	2.4	0.0281	1.6295	2.5	0.1460	0.7869	2.7	0.1546	0.6982
Parameters of actual curves of flow															
			Bingham		Casson		generalized Casson			Herschel–Bulkley			Vočadlo		
W/C	C_s	C_V	τ_{0B}	η_{pl}	τ_{0C}	η_C	τ_{0Cg}	η_{Cg}	n	τ_{0HB}	K_{HB}	n	τ_{0V}	K_V	n
	[%]	[%]	[Pa]	[Pa·s]	[Pa]	[Pa·s]	[Pa·s]	[Pa]	[–]	[Pa]	[Pa·s^n]	[–]	[Pa]	[Pa·s^n]	[–]
0.35	74.1	48.0	46.1	0.4360	24.5	0.2264	21.4	0.1967	2.2045	23.6	3.2060	0.6738	25.6	22.6804	0.5813
0.40	71.4	44.6	25.7	0.2890	12.4	0.1626	14.0	0.1786	1.8408	15.3	1.3066	0.7515	16.7	3.4861	0.6703
0.50	66.7	39.2	11.8	0.1357	5.6	0.0777	7.6	0.0982	1.5895	8.1	0.4536	0.8009	8.6	0.7354	0.7196
0.60	62.5	35.0	6.6	0.0656	3.2	0.0360	4.4	0.0471	1.5626	4.6	0.2347	0.7911	4.8	0.3306	0.6942
0.70	58.8	31.6	3.2	0.0384	1.5	0.0223	2.3	0.0303	1.4489	2.4	0.1017	0.8387	2.5	0.0993	0.7646

Table 2.4

Rheological parameters of apparent and actual curves of flow of cement pastes made from cement CEM II/B-S 42.5 N, detemined basing on various rheological models

Parameters of apparent curves of flow															
			Bingham		Casson		generalized Casson			Herschel–Bulkley			Vočadlo		
W/C	C_s [%]	C_V [%]	τ_{0B} [Pa]	η_{pl} [Pa·s]	τ_{0C} [Pa]	η_C [Pa·s]	τ_{0Cg} [Pa·s]	η_{Cg} [Pa]	n [–]	τ_{0HB} [Pa]	K_{HB} [Pa·s^n]	n [–]	τ_{0V} [Pa]	K_V [Pa·s^n]	n [–]
0.40	71.4	44.6	58.4	0.5861	31.5	0.2983	1.0	0.0081	7.0728	21.8	9.1788	0.5479	20.0	124.214	0.5122
0.50	66.7	39.2	27.8	0.2995	14.6	0.1568	9.8	0.1058	2.5825	13.5	2.2514	0.6635	15.8	10.5332	0.5831
0.60	62.5	35.0	11.4	0.1081	6.2	0.0541	6.3	0.0553	1.9683	7.4	0.5598	0.7246	8.3	1.2420	0.6240
0.70	58.8	31.6	8.0	0.0744	4.4	0.0367	3.7	0.0293	2.3069	4.6	0.5226	0.6749	5.3	1.0834	0.5768
Parameters of actual curves of flow															
			Bingham		Casson		generalized Casson			Herschel–Bulkley			Vočadlo		
W/C	C_s [%]	C_V [%]	τ_{0B} [Pa]	η_{pl} [Pa·s]	τ_{0C} [Pa]	η_C [Pa·s]	τ_{0Cg} [Pa·s]	η_{Cg} [Pa]	n [–]	τ_{0HB} [Pa]	K_{HB} [Pa·s^n]	n [–]	τ_{0V} [Pa]	K_V [Pa·s^n]	n [–]
0.40	71.4	44.6	58.1	0.4816	31.3	0.2456	1.4	0.0094	6.6202	22.6	8.0017	0.5524	20.3	96.893	0.5147
0.50	66.7	39.2	25.6	0.2705	12.5	0.1499	10.7	0.1319	2.2120	13.8	1.5331	0.7158	15.7	4.5867	0.6387
0.60	62.5	35.0	10.5	0.0971	5.2	0.0525	5.8	0.0574	1.8569	6.9	0.4204	0.7607	7.7	0.6938	0.6746
0.70	58.8	31.6	7.5	0.0656	3.8	0.0345	3.3	0.0296	2.2195	4.2	0.4050	0.7045	4.9	0.6377	0.6176

2.4. Selected rheological model

During the approximation of measurement points with use of various models, as specified in section 2.3, the following statistical parameters were also calculated:
– coefficient of determination R^2

$$R^2 = 1 - \frac{\sum_{i=1}^{n_m} \left(\tau_i - \hat{\tau}_i\right)^2}{\sum \left(\tau_i - \overline{\tau}\right)} \tag{2.1}$$

– residual sum of squares *RSS*

$$RSS = \sum_{i=1}^{n_m} \left(\tau_i - \hat{\tau}_i\right)^2 \tag{2.2}$$

– residual standard error *RSE*

$$RSE = \sqrt{\frac{\sum_{i=1}^{n_m} \left(\tau_i - \hat{\tau}_i\right)^2}{n_m - n_p}} \tag{2.3}$$

Where:

τ_i – actual value of stress (adjusted due to the non-Newtonian nature of the mixture),

$\hat{\tau}_i$ – value of stress calculated on the basis of the given rheological model,

$\overline{\tau}_i$ – arithmetic average of the actual stress values,

n_m – number of the approximated measurement points,

n_p – number of rheological parameters in the given model.

The resulting calculated statistical parameters for specific rheological models are presented in Table 2.5, and Figures 2.7, 2.8 present the variability of the relative standard error *RSE* depending on the water to cement ratio *W/C*, mass concentration C_s and volume concentration C_V, for the approximation of the actual curves of flow with use of various rheological models.

The analysis of the data presented in Table 2.5 and in Figures 2.7, 2.8 reveals that for most tested concentrations the rheological models were best aligned with the obtained measurement results in the case when the tri-parametric Herschel–Bulkley model was applied (1.4). Thus, the Herschel–Bulkley model was adopted for the purposes of further application in this monograph.

Table 2.5

Statistical parameters of actual curves of flow of cement pastes, determined basig on various rheological models

CEM II/B-S 32.5 R																
			Bingham			Casson			generalized Casson			Herschel–Bulkley			Vočadlo		
W/C	C_s [%]	C_V [%]	R^2	RSS [Pa^2]	RSE [Pa]	R^2	RSS [Pa^2]	RSE [Pa]	R^2	RSS [Pa^2]	RSE [Pa]	R^2	RSS [Pa^2]	RSE [Pa]	R^2	RSS [Pa^2]	RSE [Pa]
0.35	74.1	48.0	0.9795	1259	6.59	0.9978	136.30	2.17	0.9980	122.42	2.09	0.9978	133.14	2.18	0.9971	178.41	2.52
0.40	71.4	44.6	0.9894	265.4	3.03	0.9992	19.36	0.82	0.9994	15.74	0.75	0.9994	14.70	0.72	0.9990	24.57	0.94
0.50	66.7	39.2	0.9936	34.96	1.10	0.9984	8.68	0.55	0.9996	2.30	0.29	0.9998	1.02	0.19	0.9997	1.50	0.23
0.60	62.5	35.0	0.9914	11.68	0.63	0.9963	5.02	0.42	0.9979	2.82	0.32	0.9988	1.56	0.24	0.9994	0.83	0.17
0.70	58.8	31.6	0.9958	1.76	0.24	0.9973	1.13	0.20	0.9996	0.15	0.07	0.9997	0.12	0.06	0.9996	0.16	0.08
CEM II/B-S 42.5 N																	
			Bingham			Casson			generalized Casson			Herschel–Bulkley			Vočadlo		
W/C	C_s [%]	C_V [%]	R^2	RSS [Pa^2]	RSE [Pa]	R^2	RSS [Pa^2]	RSE [Pa]	R^2	RSS [Pa^2]	RSE [Pa]	R^2	RSS [Pa^2]	RSE [Pa]	R^2	RSS [Pa^2]	RSE [Pa]
0.40	71.4	44.6	0.9629	3277	10.63	0.9919	713.87	4.96	0.9988	105.87	1.94	0.9990	85.58	1.75	0.9991	71.40	1.60
0.50	66.7	39.2	0.9869	296.5	3.20	0.9995	12.01	0.64	0.9996	9.29	0.58	0.9996	8.87	0.56	0.9993	15.40	0.74
0.60	62.5	35.0	0.9919	23.62	0.90	0.9996	1.04	0.19	0.9997	0.85	0.17	0.9998	0.87	0.18	0.9993	1.36	0.22
0.70	58.8	31.6	0.9867	18.53	0.80	0.9995	0.69	0.15	0.9996	0.52	0.13	0.9997	0.43	0.12	0.9995	0.70	0.16

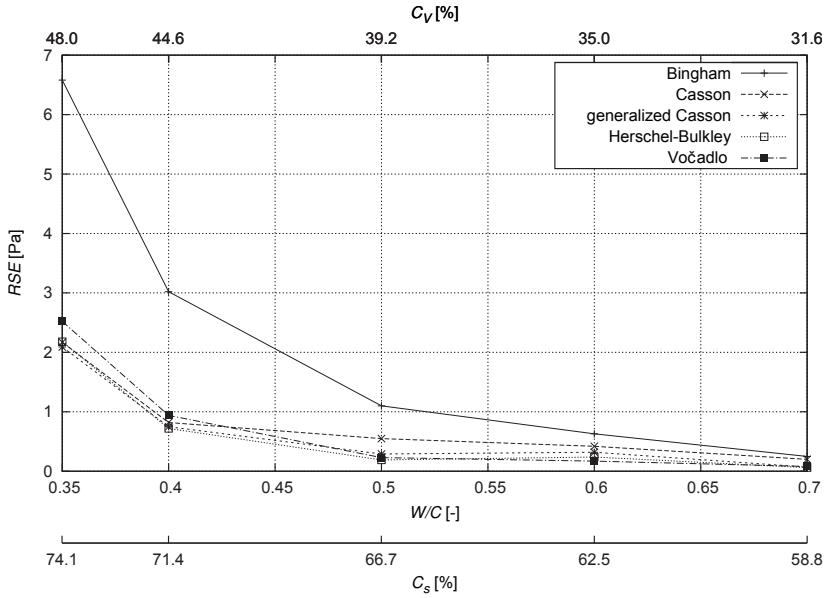

Fig. 2.7. Residual standard error *RSE* calculated with use of the approximation of the actual curves of flow of cement pastes made from cement CEM II/B-S 32.5 R by various rheological models

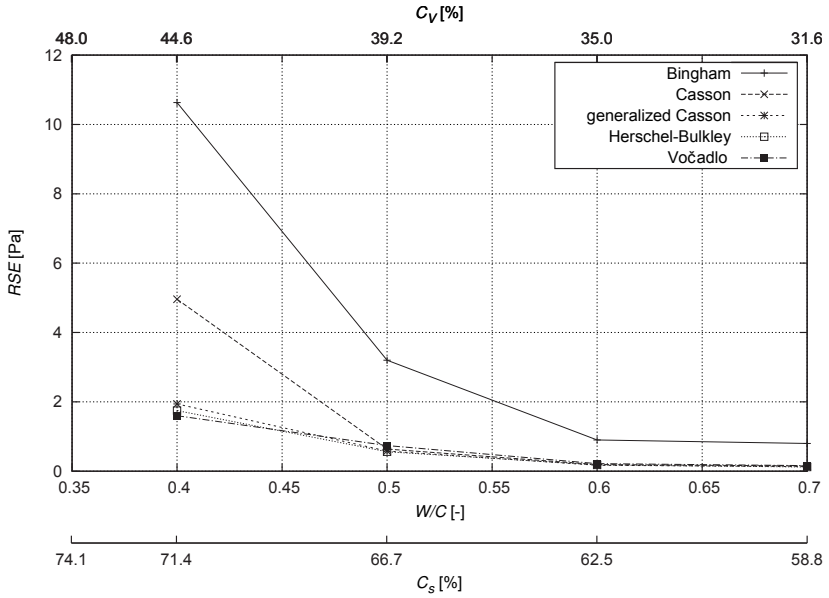

Fig. 2.8. Residual standard error *RSE* calculated with use of the approximation of the actual curves of flow of cement pastes made from cement CEM II/B-S 42.5 N by various rheological models

2.5. Analysis of test results

The subject of the analysis were the actual curves of flow, approximated with use of the Herschel–Bulkley model (1.4), presented in Figures 2.9, 2.10.

Figure 2.11 shows the variability of the value of yield stress τ_{0HB}, calculated for the Herschel–Bulkley model (1.4), as a function of the water to cement ratio *W/C*, mass concentration C_s and volume concentration C_V of the tested cement pastes. The values of yield stress for the tested range of concentrations of cement pastes fluctuated: for CEM II/B-S 32.5 R within the range from 2.4 Pa to 23.6 Pa (at *W/C* rate varying, respectively, from 0.7 do 0.35), and for cement CEM II/B-S 42.5 N within the range from 4.2 Pa to 22.2 Pa (at *W/C* rate varying, respectively, from 0.7 do 0.4). As expected, the calculated values of the yield stress decreased with the increase in water to cement ratio, i.e., they increased with the increase of mass and volume concentrations and were visibly higher for pastes made from cement CEM II/B-S 42.5 N. The nature of the changes in yield stress for the tested range of variability of water to cement ratio *W/C* can be described with use of power functions (2.4) and (2.5).

– for cement CEM II/B-S 32.5 R

$$\tau_{0HB} = -0.403059 + 1.05147\left(W/C\right)^{-2.97411} \tag{2.4}$$

– for cement CEM II/B-S 42.5 N

$$\tau_{0HB} = -12.5601 + 10.1631\left(W/C\right)^{-1.34569} \tag{2.5}$$

The relation between the consistency index K_{HB} and the water to cement ratio *W/C*, mass concentration C_s and volume concentration C_V is presented in Figure 2.12. For the analysed range of concentration of cement pastes, the values of this index changed in the range from 0.1017 Pa·s^n to 3.2060 Pa·s^n for cement CEM II/B-S 32.5 R (*W/C* ranged from 0.7 to 0.35) and in the range from 0.4050 Pa·s^n to 5.7300 Pa·s^n for cement CEM II/B-S 42.5 N (*W/C* ranged from 0.7 to 0.4). Similarly to the case of the yield stress, also the values of the consistency index, calculated with use of the Herschel–Bulkley model, noticeably decreased with the increase of the water to cement ratio, i.e. increased with the increase of mass or volume concentration. Here again, higher values were recorded for cement CEM II/B-S 42.5 N. The nature of the changes in the consistency index for the analysed range of the *W/C* ratio of cement pastes can be described with use of the equations (2.6) and (2.7).

– for cement CEM II/B-S 32.5 R

$$K_{HB} = 5.55626 \cdot 10^{-3}\left(W/C\right)^{-6.04619} \tag{2.6}$$

– for cement CEM II/B-S 42.5 N

$$K_{HB} = 25.75 \cdot 10^{-3}\left(W/C\right)^{-5.89836} \tag{2.7}$$

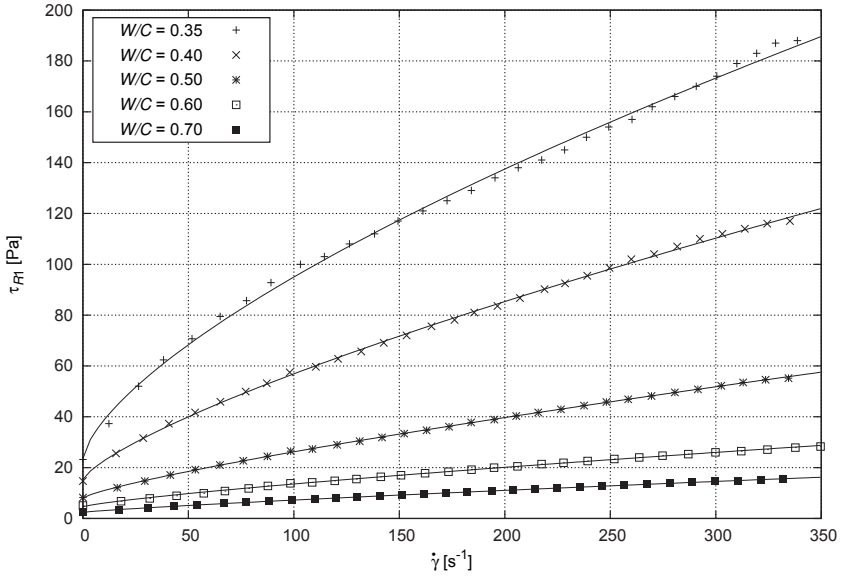

Fig. 2.9. Actual curves of flow of the tested cement pastes made from cement CEM II/B-S 32.5 R and their approximation with use of the Herschel–Bulkley model

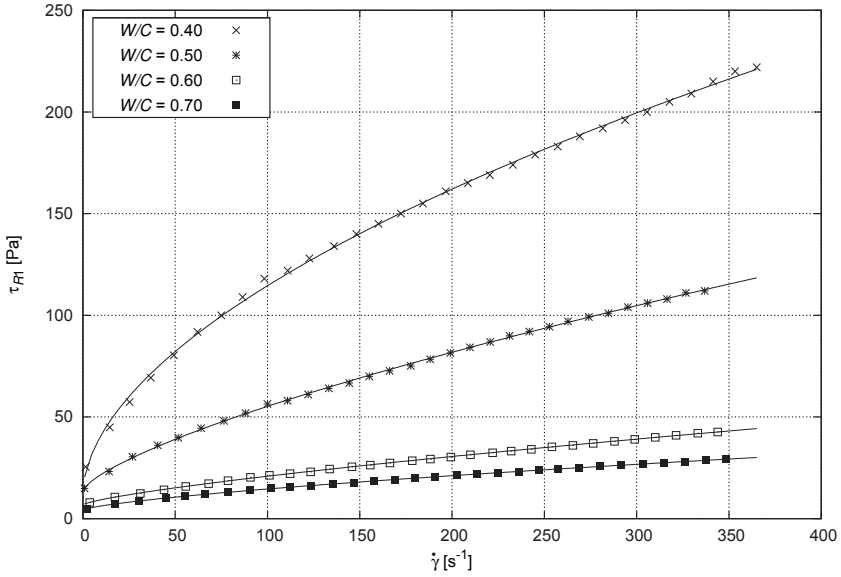

Fig. 2.10. Actual curves of flow of the tested cement pastes made from cement CEM II/B-S 42.5 N and their approximation with use of the Herschel–Bulkley model

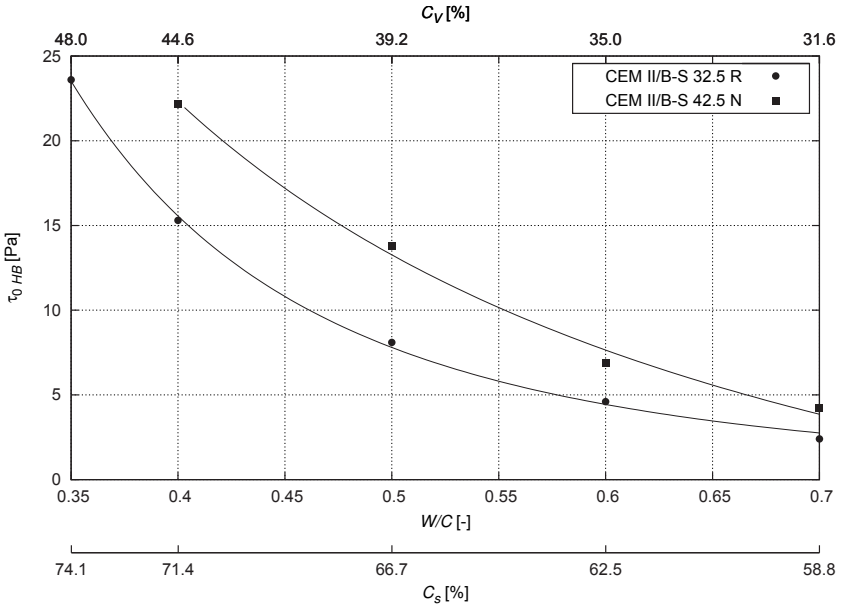

Fig. 2.11. Relation between the yield stress τ_{0HB} calculated for the Herschel–Bulkley model, and water to cement ratio *W/C*, mass concentration C_s and volume concentration C_V

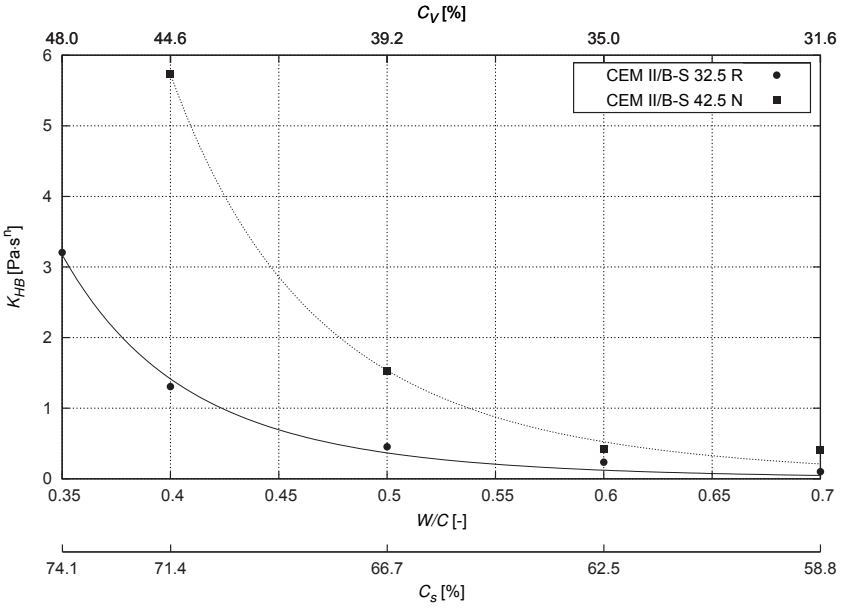

Fig. 2.12. Relation between the consistency index K_{HB} calculated for the Herschel–Bulkley model, and water to cement ratio *W/C*, mass concentration C_s and volume concentration C_V

Figure 2.13 presents the changes in the flow behaviour index n in the Herschel–Bulkley model as a function of water to cement ratio *W/C*, mass concentration C_s and volume concentration C_V. The values of the flow behaviour index *n* for the tested concentrations of pastes fluctuated within the range from 0.6738 to 0.8387 for cement CEM II/B-S 32.5 R (*W/C* respectively 0.7 – 0.35) and within the range from 0.6020 to 0.7045 for cement CEM II/B-S 42.5 N (*W/C* respectively 0.7 – 0.4). It was noted that the flow behaviour index increased with the increase of the water to cement ratio *W/C* of the tested pastes, although in the case of flow behaviour index higher values were recorded for cement CEM II/B-S 32.5 R. This means that the index decreases with the increase of mass concentration C_s and volume concentration C_V. The nature of the changes of the flow behaviour index *n* in relation to water to cement ratio *W/C* can be described with equations (2.8) and (2.9).

– for cement CEM II/B-S 32.5 R

$$n = -1.49205 + 2.40958\left(W/C\right)^{0.0885817} \tag{2.8}$$

– for cement CEM II/B-S 42.5 N

$$n = -7.37455 + 8.19755\left(W/C\right)^{0.0252864} \tag{2.9}$$

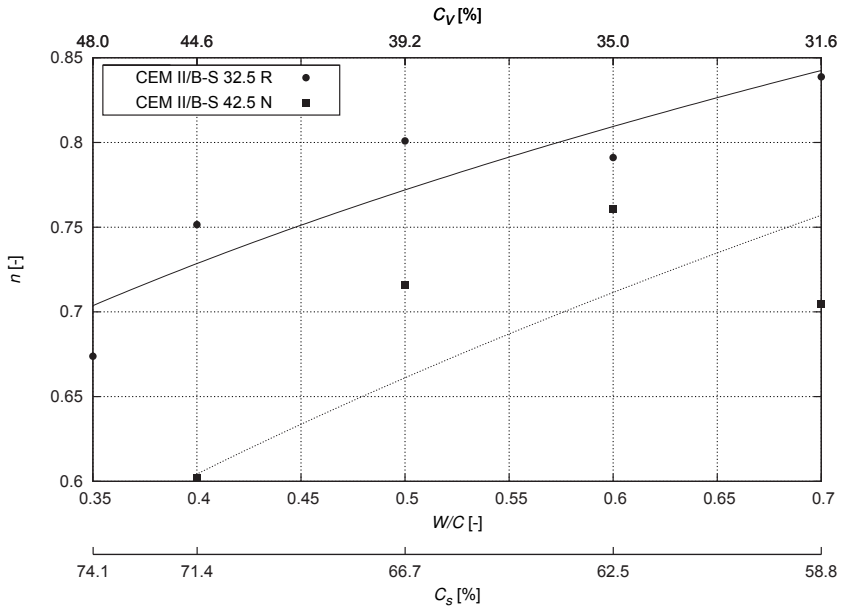

Fig. 2.13. Relation between the flow behaviour index *n* calculated for the Herschel–Bulkley model, and the water to cement ratio *W/C*, mass concentration C_s and volume concentration C_V

3. BOUNDARY PARAMETERS OF LAMINAR FLOW DURING PIPE TRANSPORT

Description of the laminar flow in a pipeline requires the determination of basic parameters that determine such flow and, eventually, enable to define it precisely. These parameters are: marginal concentration $C_{s,\lim}$, transient velocity v_{gr}, critical Reynolds number Re_{kr}, critical velocity v_{kr}, Darcy friction factor λ.

3.1. Marginal concentration

Marginal mass concentration $C_{s,\lim}$ or volume concentration $C_{V,\lim}$ is defined as such content of solid substance in a mixture, below which the behaviour of the mixture can be described as Newtonian, and above – as non-Newtonian [5, 16, 23].

In the case of the Herschel–Bulkley model, the transition from non-Newtonian to Newtonian behaviour occurs at $n = 1$ and $\tau_0 = 0$.

The methodology of determination of the marginal concentration on the basis of viscometric measurements in the non-Newtonian zone was suggested by Czaban [5]. The determination of the marginal concentration requires an approximation of the changes in n and τ_0 as a function of concentration, by the following equation:

$$y = b_0 + b_1 C_s^{b_2} \tag{3.1}$$

Then, the value of marginal concentration should be determined:

– for $\tau_0 = 0$:

$$C_{s,\lim 1} = \left(-\frac{b_0}{b_1} \right)^{\frac{1}{b_2}} \tag{3.2}$$

– for $n = 1$:

$$C_{s,\lim 2} = \left(\frac{1 - b_0}{b_1} \right)^{\frac{1}{b_2}} \tag{3.3}$$

The lower value of the two calculated as a result of equations (3.2) and (3.3) is considered as the marginal concentration.

For the tested cement pastes, the relations describing the variability of the values τ_0 and n as a function of the water to cement ratio W/C, and thus of mass concentration C_s and volume concentration C_V, have the form of equations (2.4) and (2.5), as well as (2.8) and (2.9).

Basing on the parameters of the equations (2.4) and (2.5) as well as (2.8) and (2.9), and the relations (3.2) and (3.3), the following values of marginal concentration were determined for the tested pastes made from cement CEM II/B-S 32.5 R:

- for $\tau_0 = 0$: $(W/C)_{lim1} = 1.38$, $C_{s,lim1} = 42.0\%$, $C_{V,lim1} = 19.1\%$;
- for $n = 1$: $(W/C)_{lim2} = 1.46$, $C_{s,lim2} = 40.6\%$, $C_{V,lim2} = 18.2\%$.

and for pastes made from cement CEM II/B-S 42.5 N:

- for $\tau_0 = 0$: $(W/C)_{lim1} = 0.86$, $C_{s,lim1} = 53.8\%$, $C_{V,lim1} = 27.3\%$;
- for $n = 1$: $(W/C)_{lim2} = 2.33$, $C_{s,lim2} = 30.0\%$, $C_{V,lim2} = 12.2\%$.

All tested mixtures of cement pastes were characterised by concentrations higher than marginal concentrations C_s i C_V and values of water to cement ratio W/C lower than marginal. Thus, they were non-Newtonian mixtures in the whole tested range.

3.2. Minimal transient velocity in horizontal pipelines

Transient velocity v_{gr} is the minimal velocity that enables the floating of solid particles in the mix. Below transient velocity, massive fallout and sedimentation of solid particles occur, and sediment is created on the bottom of the pipeline. Transient velocity is determined by means of direct observation in a transparent pipeline, or indirectly, as a result of the analysis of parameters of flow presented in form of a relation $I(v)$, or the observation of the sedimentation process in sedimentation columns that enable to determine the sedimentation rate $w(C_s)$.

In order to analyse this phenomenon, mean sedimentation rate was tested in sedimentation columns of cement pastes characterised by water to cement ratio W/C ranging from 0.4 to 0.7. The results of the determination are listed in Table 3.1 and presented in graphic form in Figures 3.1 and 3.2. It was determined that the mean sedimentation rate noticeably increases with the increase of the water to cement ratio W/C, i.e. that it decreases with the increase of the concentration of mixtures (Fig. 3.3). The nature of the changes for the tested measurement scope can be described by the following relations:

– for cement CEM II/B-S 32.5 R

$$w = 9.41 \cdot 10^{-7} + 1.40 \cdot 10^{-4} \left(W/C\right)^{8.374} \tag{3.4}$$

– for cement CEM II/B-S 42.5 N

$$w = 8.72 \cdot 10^{-7} + 5.79 \cdot 10^{-5} \left(W/C\right)^{7.920} \tag{3.5}$$

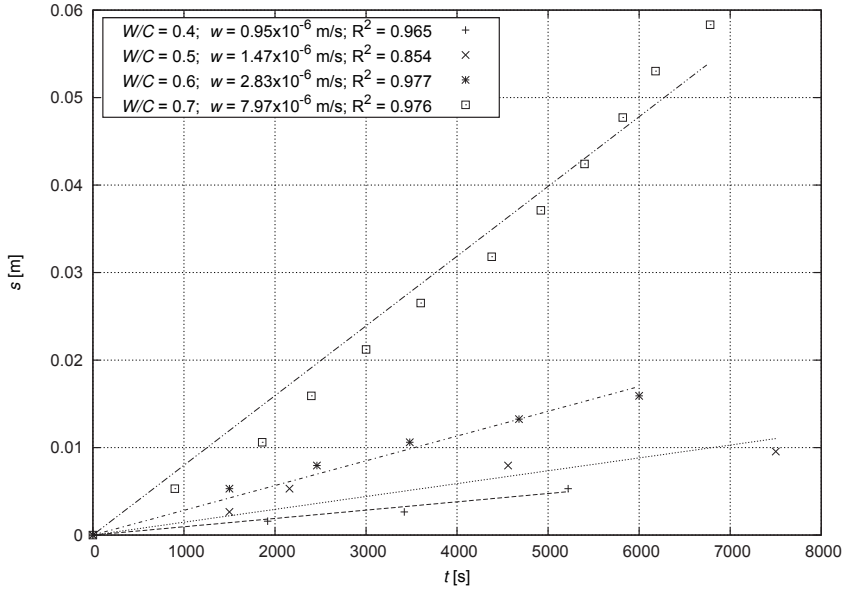

Fig. 3.1. Results of tests of sedimentation rate *w* of cement pastes made from cement CEM II/B-S 32.5 R

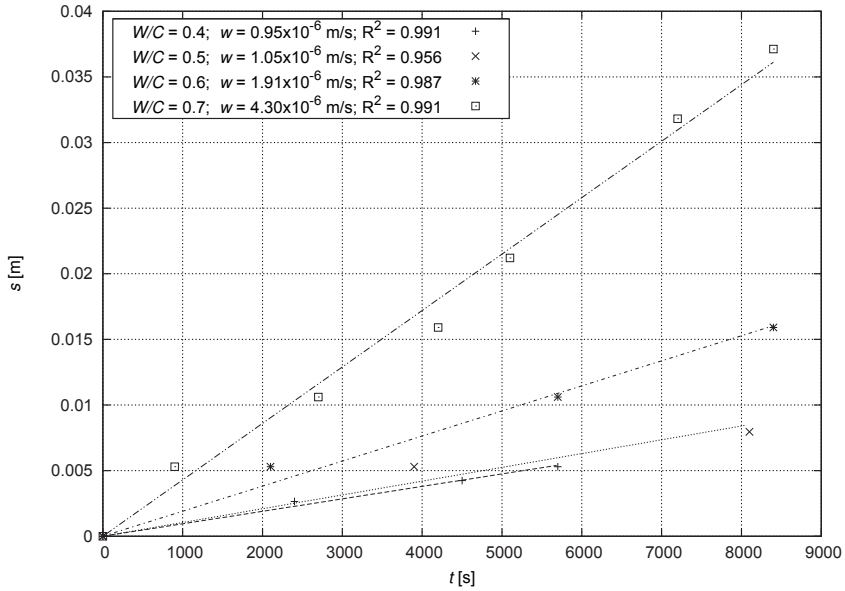

Fig. 3.2. Results of tests of sedimentation rate *w* of cement pastes made from cement CEM II/B-S 42.5 N

Transient velocity $v_{gr,}$ defined by Newitt as the minimal velocity at which the suspension moves from homogenous to heterogeneous state, was calculated according to the proportion (3.6), basing on the previously calculated mean sedimentation rates w (Table 3.1).

Table 3.1

Results of the tests of mean sedimentation rate w of pastes made with use of the tested cements, with the respective values of transient velocity v_{gr} calculated according to the proportion (3.6)

W/C [−]	C_s [%]	C_V [%]	w [m·s^{-1}]×10^{-6}	v_{gr} [m·s^{-1}], for D [mm]				
				20	30	40	50	60
CEM II/B-S 32.5 R								
0.40	71.4	44.6	0.93	0.069	0.079	0.087	0.094	0.100
0.50	66.7	39.2	1.47	0.080	0.092	0.101	0.109	0.116
0.60	62.5	35.0	2.83	0.100	0.114	0.126	0.136	0.144
0.70	58.8	31.6	7.97	0.141	0.162	0.178	0.192	0.204
CEM II/B-S 42.5 N								
0.40	71.4	44.6	0.95	0.070	0.080	0.088	0.094	0.100
0.50	66.7	39.2	1.05	0.072	0.082	0.091	0.098	0.104
0.60	62.5	35.0	1.91	0.088	0.100	0.110	0.119	0.126
0.70	58.8	31.6	4.30	0.115	0.132	0.145	0.156	0.166

$$v_{gr} = \left(1800 g D w\right)^{\frac{1}{3}} \tag{3.6}$$

Where:
D – pipe diameter [m];
w – mean sedimentation rate [m·s^{-1}];
g – acceleration of gravity [m·s^{-2}]

The results of calculations of the transient velocity, according to equation (3.6) are listed in Table 3.1 and presented in graphic form in Figures 3.4 and 3.5.

The value of transient velocity is influenced by the type of transported mix (the density and shape of solid particles, granulation curves, volume or mass concentration, rheological properties). The theoretical basis for the determination of transient velocity in pipelines, for the flow of mixture of sand and water, was presented by Durand. Further studies in this area were conducted by Gibert, Smith, Charles, Stevens, Silin and others [23].

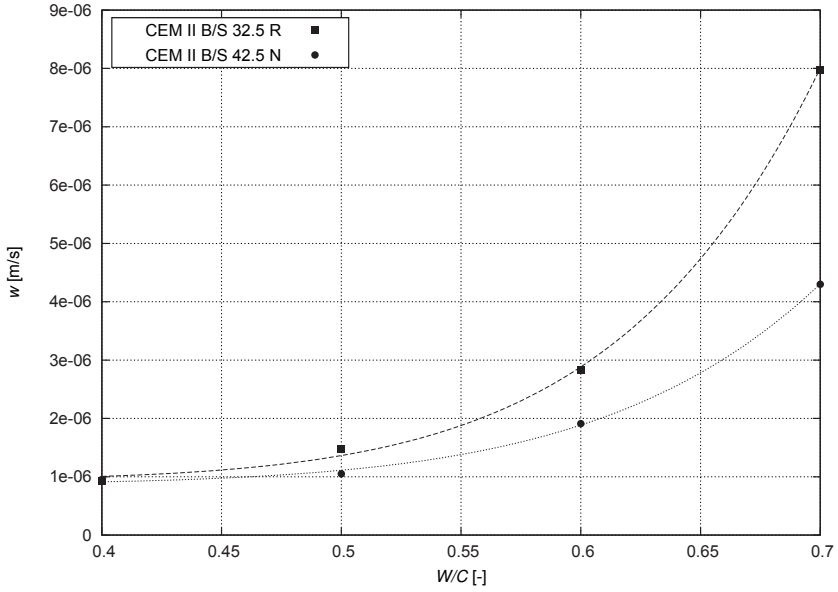

Fig. 3.3. The relation between the mean sedimentation rate and the water to cement ratio *W/C* of pastes made with use of the tested cements

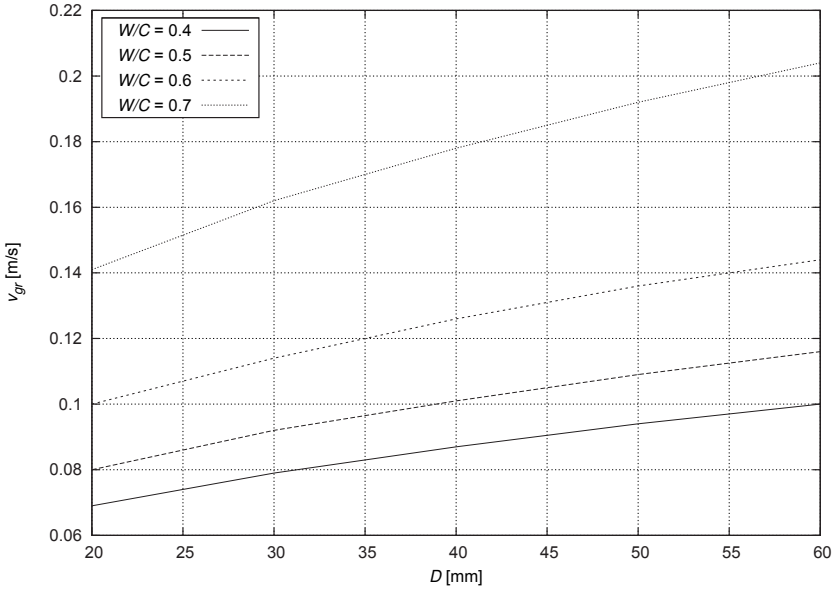

Fig. 3.4. The relation between the transient velocity v_{gr}, calculated with use of proportion (3.6), and the pipe diameter *D* and the water to cement ratio *W/C* of pastes made with use of cement CEM II/B-S 32.5 R

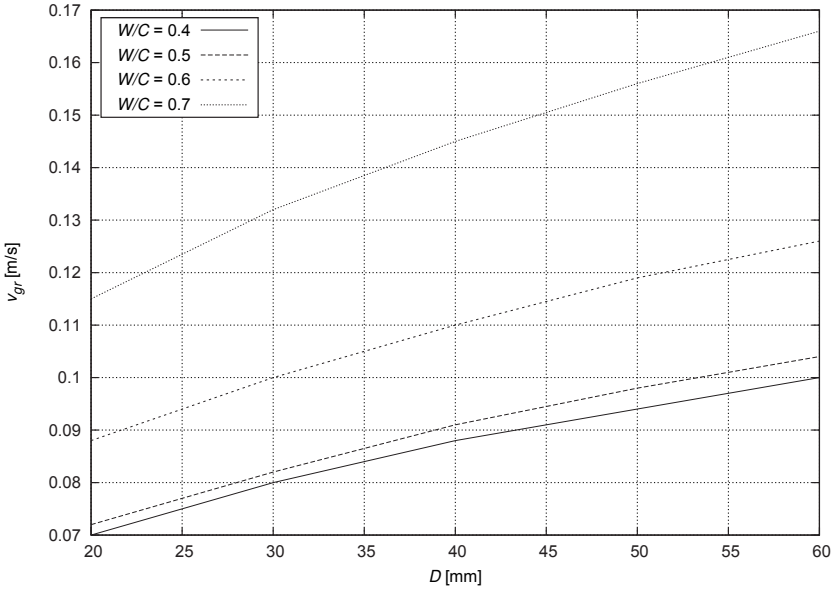

Fig. 3.5. The relation between the transient velocity v_{gr}, calculated with use of proportion (3.6), and the pipe diameter D and the water to cement ratio W/C of pastes made with use of cement CEM II/B-S 42.5 N

Durand proposed the following general structural formula for the determination of transient velocity of heterogeneous mixtures:

$$v_{gr} = f\left(\rho_s, \rho_w, D, C_V, g, d\right) \tag{3.7}$$

For homogeneous and quasi-homogeneous mixtures the above formula needs to be modified to the following form:

$$v_{gr} = f\left(\rho_s, \rho_m, D, C_V, g, \eta_m\right) \tag{3.8}$$

Considering the above, the Durand formula for such heterogeneous mixtures as sand particles and water, adopts the following form:

$$v_{gr} = F_L\left[2gD\frac{\left(\rho_s - \rho_w\right)}{\rho_w}\right]^{0.5} \tag{3.9}$$

Whereas for homogeneous mixtures:

$$v_{gr} = F_L \left[2gD \frac{(\rho_s - \rho_m)}{\rho_m} \right]^{0.5} \tag{3.10}$$

where F_L is a non-dimensional parameter depending, among others, on the pipe diameter and type of mixture. According to Durand, for mixture of sand and gravel F_L fluctuates within the range 0.65–1.15, while for homogeneous or quasi-homogeneous mixtures (organic sediments, liquid manure) F_L fluctuates within the range 0.2–0.5. For high concentrations, nearing thixotropic concentration, the value of F_L approaches zero [8].

Basing on the transient velocity values calculated with use of the proportion (3.6) and the transformed proportion (3.10), the values of the F_L parameter were determined for tested cement pastes. The obtained values of the F_L parameter varied, depending on the concentration of the tested mixtures and the pipe diameter D, within the range from 0.082 to 0.249 for cement CEM II/B-S 32.5 R (Fig. 3.6) and from 0.079 to 0.197, for cement CEM II/B-S 42.5 N (Fig. 3.7).

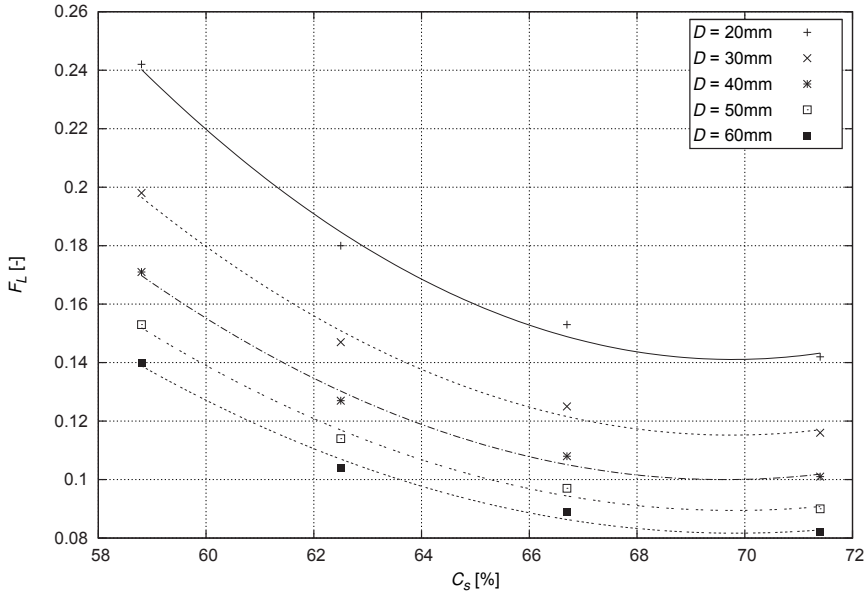

Fig. 3.6. The relation between the parameter F_L and mass concentration C_s, for different pipe diameters D. Paste made with use of cement CEM II/B-S 32.5 R

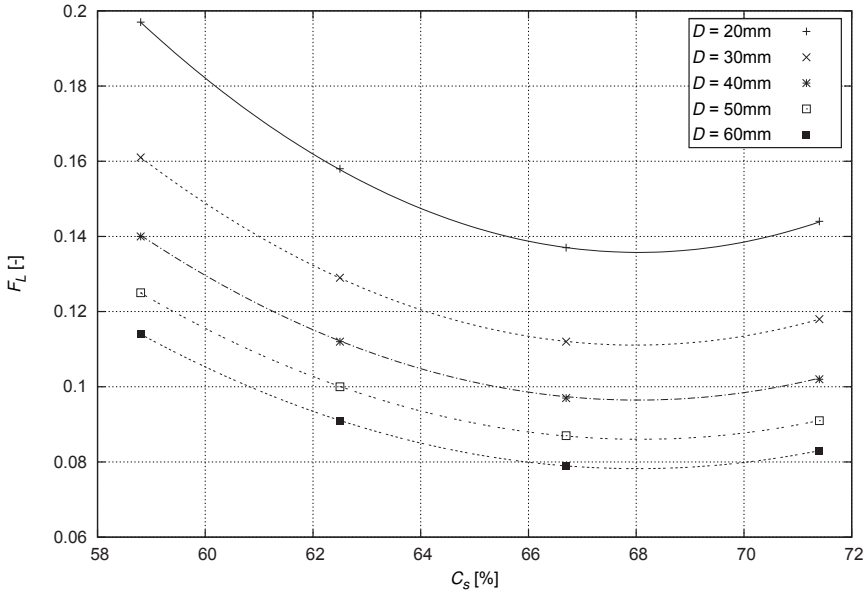

Fig. 3.7. The relation between the parameter F_L and mass concentration C_s, for different pipe diameters D. Paste made with use of cement CEM II/B-S 42.5 N

3.3. Laminar flow in the pipe

Hydraulic flow takes the form of one of three basic regimens of flow: laminar, transitional and turbulent. The regimen of flow is determined by the diameter of the designed pipe D, volumetric flow rate Q, physical, chemical and rheological properties of the transported mixture.

The parameter that characterises the regimen of flow is Reynolds number Re. The critical value of Reynolds number, limiting the laminar flow, falls, for Newtonian liquids, into the range $Re_{kr} = 2100-2320$ [7, 23, 31]. Pipe flows of Newtonian liquids characterised by a Reynolds number $Re \leq 2300$ belong to the category of laminar flows. Reynolds number for Newtonian bodies is generally known and presented in the form of the proportion:

$$Re = \frac{vD\rho}{\eta} \tag{3.11}$$

where:
v – mean flow rate [m·s^{-1}];
D – pipe diameter [m];
η – viscosity of the liquid [Pa·s];
ρ – density of the liquid [kg·m^{-3}];

For non-Newtonian liquids the formula for calculating the Reynolds number results from the adopted rheological model. The authors consider it justified to use, for the purpose of description of flow of the tested cement pastes, the general, tri-parametric rheological Herschel–Bulkley model (1.4). As a general model it encompasses simpler, bi-parametric and single-parameter models, through the adoption of $n = 1$ (transformation to the Bingham model (1.1), $K_{HB} = \eta_{pl}$) and $\tau_0 = 0$ (transition to Newton model $K_{HB} = \eta$).

The complete, general Reynolds number for the Herschel–Bulkley model has been proposed by one of the authors [17] in the following form:

$$Re_{H,gen} = \frac{8v^{(2-n)}D^n\rho}{2^n k} \cdot \left\{ \frac{n}{n+1}\left(1-\frac{\tau_0}{\tau_w}\right)^{\frac{n+1}{n}}\left[1-\frac{2n}{3n+1}\left(1-\frac{\tau_0}{\tau_w}\right)\left(1+\frac{n}{2n+1}\frac{\tau_0}{\tau_w}\right)\right]\right\}^n \tag{3.12}$$

where:
v – mean flow rate [m·s^{-1}];
D – pipe diameter [m];
ρ – density of the liquid [kg·m^{-3}];
τ_w – stress on pipe wall [Pa];
τ_0, k, n – parameters of the Herschel–Bulkley model (1.4).

This is also a general Reynolds number, which can be simplified to Reynolds numbers of simpler models. For example, for the bi-parametric Bingham model describing viscoplastic mixtures, with a constant plastic viscosity η_{pl}, the formula will take the following form:

$$Re_B = \frac{vD\rho}{\eta_{pl}}\left[1-\frac{4}{3}\frac{\tau_0}{\tau_w}+\frac{1}{3}\left(\frac{\tau_0}{\tau_w}\right)^4\right] \tag{3.13}$$

This is the full Reynolds number in the Bingham model, which replaces simplified forms presented in literature that do not take into account the tangent stress on the wall of the pipe.

The value of the tangent stress τ_w for the adopted rheological model should be calculated on the basis of previously determined rheological parameters and flow parameters (D, v). The presented formula (3.14) [17] for the Herschel–Bulkley model is also general and can be simplified to simpler formulas.

$$\tau_w = \frac{(2v)^n k}{D^n \left\{ \frac{n}{n+1}\left(1-\frac{\tau_0}{\tau_w}\right)^{\frac{n+1}{n}} \left[1-\frac{2n}{3n+1}\left(1-\frac{\tau_0}{\tau_w}\right)\left(1+\frac{n}{2n+1}\frac{\tau_0}{\tau_w}\right)\right]\right\}^n} \tag{3.14}$$

The determination of the values of tangent stresses τ_w with use of formula (3.14) requires the calculation, by means of subsequent approximations, by substitution of the subsequent values $\tau_w > \tau_0$, until the point when the equation is met.

3.4. Determination of the critical Reynolds number Re_{kr}

Ryan and Johnson [26] had analysed the variability of the function determining the stability number Z_R and presented the theoretical basis for the determination of the critical Reynolds number Re_{kr}. Czaban [5] has used the above described method in order to determine the formula (3.15) for the calculation of general critical Reynolds number for the Herschel–Bulkley model, assuming that its value equals 2300 for Newtonian liquids.

$$Re_{H,kr} = \left[\frac{110.64 \cdot 8^{\frac{4}{n}} (2+n)^{\frac{2+n}{1+n}}}{\lambda^{\frac{2-n}{n}} \left(1-\frac{\tau_0}{\tau_w}\right)^{\frac{2+n}{n}} (3n+1)^2} \right]^{\frac{n}{2}} \tag{3.15}$$

The Darcy friction factor λ in the laminar zone of flow of Newtonian liquids, described by the Herschel–Bulkley model is calculated in an analogical manner as for the liquids described by the Newtonian model, considering the general Reynolds number for this model:

$$\lambda = \frac{64}{Re_{H,gen}} \tag{3.16}$$

For the Bingham model, the formula (3.15) takes the form:

$$Re_{B,kr} = \frac{2300\left[1-\frac{4}{3}\frac{\tau_0}{\tau_w}+\frac{1}{3}\left(\frac{\tau_0}{\tau_w}\right)^4\right]}{\left(1-\frac{\tau_0}{\tau_w}\right)^3} \tag{3.17}$$

The application of the formulas presented above requires the knowledge of the shear stress on the pipe wall τ_w at the moment of transition from laminar to turbulent movement. At that point the general Reynolds number $Re_{H,gen}$ equals the general critical Reynolds number $Re_{H,kr}$.

The critical Reynolds number is determined in the following mode [17]: for the previously determined rheological parameters of the tested medium τ_0, k and n, and for the constant pipe diameter, one should:

- assume the volumetric flow rate Q and calculate, for the known pipe diameter D, the mean flow rate v;
- calculate tangent stress on the pipe wall τ_w (3.14);
- calculate the value of the Reynolds number $Re_{H,gen}$ (3.12);
- determine the Darcy friction factor λ (3.16);
- calculate the value of critical Reynolds number $Re_{H,kr}$ (3.15);
- compare the resulting values $Re_{H,gen}$ and $Re_{H,kr}$.

The algorithm for the calculation of these values is presented in Figure 3.8.

If $Re_{H,gen} < Re_{H,kr}$ the movement takes place within the adopted volumetric flow rate Q in the laminar zone. Flow rate should be increased and calculations need to be repeated.

If $Re_{H,gen} > Re_{H,kr}$ the movement takes place within the turbulent zone of the flow. Flow rate should be decreased and calculations need to be repeated.

The compatibility $Re_{H,gen} = Re_{H,kr}$ allows to determine the value of the critical Reynolds number and to calculate the value of the corresponding critical flow velocity v_{kr}.

For the tested cement pastes and the adopted diameters of feed pipe $D = 20–60$ mm the values of the critical Reynolds number $Re_{H,kr}$ and of the mean critical velocity v_{kr} were calculated. The results of these calculations are listed in Tables 3.2 and 3.3 and presented in graphic form in Figures 3.9 – 3.12. Figure 3.13 illustrates the changes in the critical Reynolds number calculated for the Herschel–Bulkley model as a function of the ratio of the yield stress to the shear stress on the pipe wall τ_0/τ_w. In the case of both tested cements, an increase in the Reynolds number with the increase in the τ_0/τ_w ratio was recorded.

Analysing the data presented in Figures 3.9 and 3.10, one can determine that the value of the critical Reynolds number $Re_{H,kr}$ noticeably decreases with the increase in the concentration of the tested mixtures, while it increases proportionally to the increase in the pipe diameter D.

As for the critical velocity v_{kr} (Fig. 3.11, Fig. 3.12), it increases proportionally to the increase in the concentration of tested mixtures and decreases with the increase in pipe diameter D.

Table 3.2

Values of critical velocity v_{kr} and corresponding critical Reynolds numbers $Re_{H,kr}$, calculated for different pipe diameters, during the flow of pastes made from cement CEM II/B-S 32.5 R

W/C	C_s [%]	C_V [%]	*D* [mm]	v_{kr} [m·s^{-1}]	$Re_{H,kr}$	τ_0/τ_w
0.35	74.1	48.0		14.49	2716	0.019
0.40	71.4	44.6		12.00	2635	0.018
0.50	66.7	39.2	20	7.55	2668	0.026
0.60	62.5	35.0		4.65	2857	0.044
0.70	58.8	31.6		3.22	2864	0.050
0.35	74.1	48.0		12.56	2812	0.028
0.40	71.4	44.6		9.84	2735	0.028
0.50	66.7	39.2	30	6.19	2818	0.041
0.60	62.5	35.0		3.97	3099	0.066
0.70	58.8	31.6		2.74	3147	0.076
0.35	74.1	48.0		10.98	2906	0.036
0.40	71.4	44.6		8.65	2837	0.038
0.50	66.7	39.2	40	5.48	2971	0.056
0.60	62.5	35.0		3.55	3290	0.082
0.70	58.8	31.6		2.54	3428	0.099
0.35	74.1	48.0		10.14	2997	0.043
0.40	71.4	44.6		7.90	2938	0.047
0.50	66.7	39.2	50	4.89	3052	0.063
0.60	62.5	35.0		3.41	3571	0.102
0.70	58.8	31.6		2.37	3703	0.120
0.35	74.1	48.0		9.55	3085	0.050
0.40	71.4	44.6		7.38	3038	0.056
0.50	66.7	39.2	60	4.75	3276	0.082
0.60	62.5	35.0		3.28	3798	0.118
0.70	58.8	31.6		2.29	3971	0.138

Table 3.3

Values of critical velocity v_{kr} and corresponding critical Reynolds numbers $Re_{H,kr}$, calculated for different pipe diameters, during the flow of pastes made from cement CEM II/B-S 42.5 N

W/C	C_s [%]	C_V [%]	*D* [mm]	v_{kr} [m·s^{-1}]	$Re_{H,kr}$	τ_0/τ_w
0.40	71.4	44.6	20	13.58	2735	0.012
0.50	66.7	39.2		11.43	2680	0.019
0.60	62.5	35.0		6.08	2830	0.038
0.70	58.8	31.6		4.59	2972	0.044
0.40	71.4	44.6	30	11.84	2789	0.016
0.50	66.7	39.2		9.52	2782	0.029
0.60	62.5	35.0		5.17	3036	0.057
0.70	58.8	31.6		4.01	3201	0.063
0.40	71.4	44.6	40	10.77	2838	0.020
0.50	66.7	39.2		8.46	2884	0.038
0.60	62.5	35.0		4.70	3238	0.073
0.70	58.8	31.6		3.70	3420	0.079
0.40	71.4	44.6	50	10.06	2884	0.023
0.50	66.7	39.2		7.77	2984	0.047
0.60	62.5	35.0		4.41	3435	0.088
0.70	58.8	31.6		3.51	3630	0.093
0.40	71.4	44.6	60	9.51	2927	0.026
0.50	66.7	39.2		7.29	3082	0.055
0.60	62.5	35.0		4.22	3627	0.101
0.70	58.8	31.6		3.39	3829	0.106

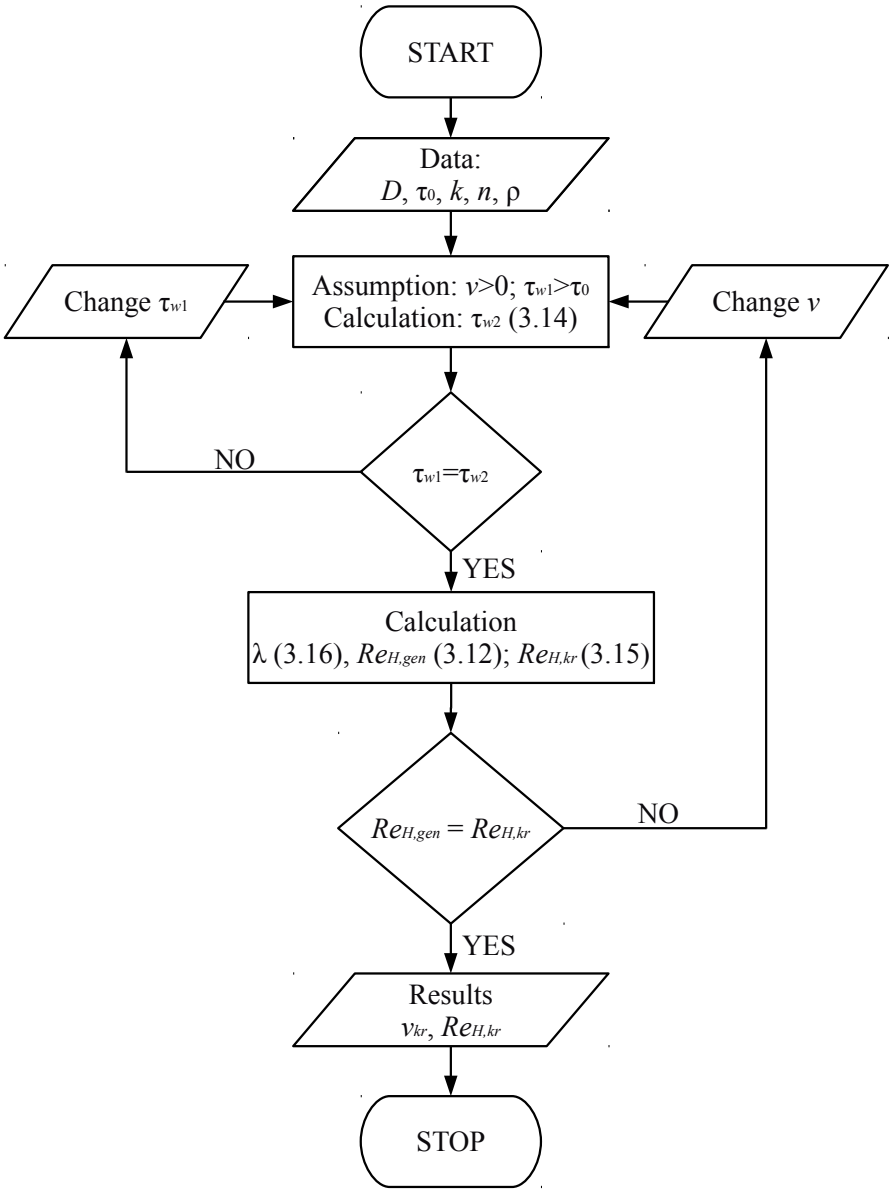

Fig. 3.8. Algorithm for the determination of critical velocity v_{kr} and of critical Reynolds number $Re_{H,kr}$

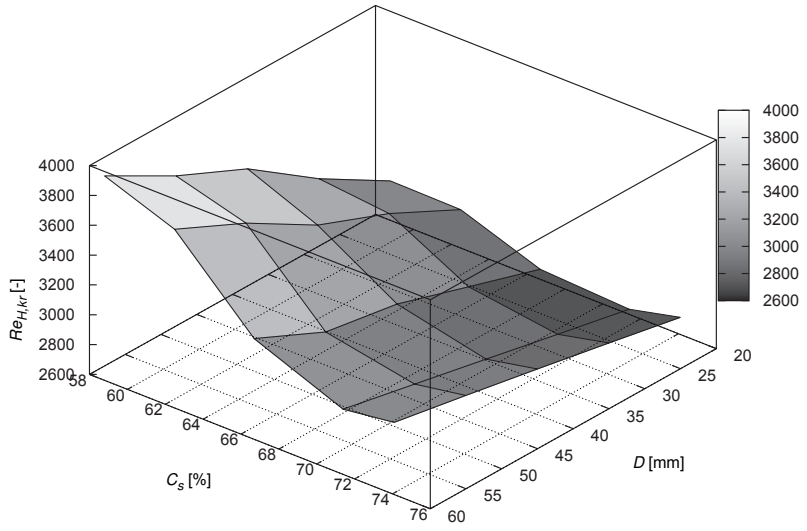

Fig. 3.9. Variability of the critical Reynolds number for the Herschel–Bulkley model $Re_{H,kr}$ of the tested cement pastes made from cement CEM II/B-S 32.5 R, as a function of mass concentration C_s and pipe diameter D

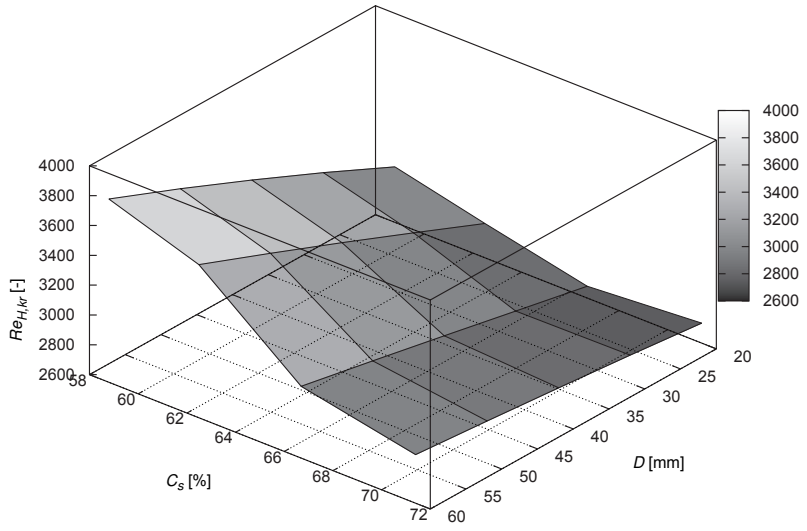

Fig. 3.10. Variability of the critical Reynolds number for the Herschel–Bulkley model $Re_{H,kr}$ of the tested cement pastes made from cement CEM II/B-S 42.5 N, as a function of mass concentration C_s and pipe diameter D

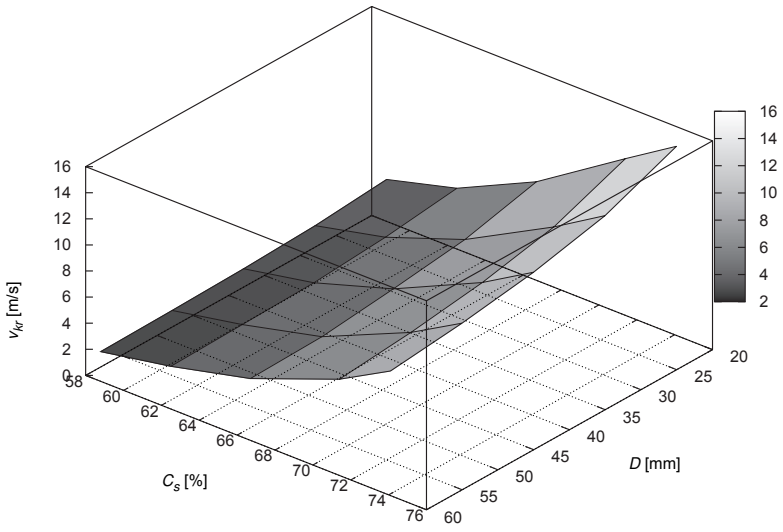

Fig. 3.11. Variability of the critical velocity v_{kr} for the Herschel–Bulkley model $Re_{H,kr}$ of the tested cement pastes made from cement CEM II/B-S 32.5 R, as a function of mass concentration C_s and pipe diameter D

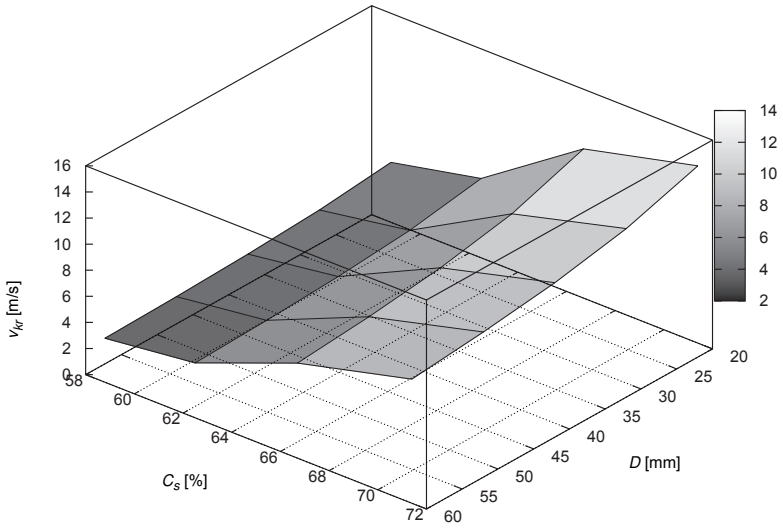

Fig. 3.12. Variability of the critical velocity v_{kr} for the Herschel–Bulkley model $Re_{H,kr}$ of the tested cement pastes made from cement CEM II/B-S 42.5 N, as a function of mass concentration C_s and pipe diameter D

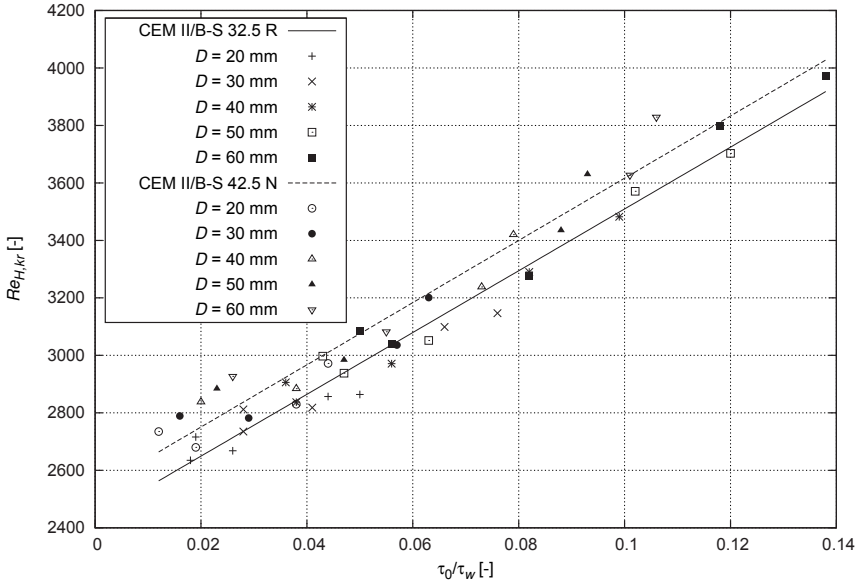

Fig. 3.13. The relation between the critical Reynolds number for the Herschel–Bulkley model $Re_{H,kr}$ and the stress quotient τ_0/τ_w

3.5. Determination of the Darcy friction factor

For the laminar zone of flow of non-Newtonian liquid, analogically to the case of Newtonian liquid, the proportion resulting from the Poiseuille equation is adopted, in the following form:

$$\lambda = \frac{64}{Re_{gen}} \tag{3.18}$$

Re_{gen} is the general Reynolds number describing the rheological properties and flow parameters of the tested medium. For example, in the Herschel–Bulkley model the general Reynolds number is determined by the relation (3.12).

The values of the Darcy friction factor λ for the analysed cement pastes are listed in Tables 3.4–3.12.

Table 3.4

Values of head loss for paste made from cement CEM II/B-S 32.5 R, $W/C = 0.35$

Q [$m^3 \cdot h^{-1}$]	v [$m \cdot s^{-1}$]	$\dot{\gamma}$ [s^{-1}]	λ [–]	h_{str} [m]	Δp [Pa]	I_m [–]
$D = 20$ mm						
0.011	0.010	4	1630.4	4.15	81805	0.42
0.170	0.150	60	16.46	9.44	185860	0.94
0.339	0.300	120	5.61	12.88	253514	1.29
0.509	0.450	180	3.05	15.72	309579	1.57
0.679	0.600	240	1.99	18.25	359397	1.83
0.893	0.750	300	1.44	20.57	405088	2.06
$D = 30$ mm						
0.025	0.010	2.67	1511.4	2.57	50556	0.26
0.573	0.225	60	7.32	6.29	123907	0.63
1.145	0.450	120	2.50	8.58	169009	0.86
1.718	0.675	180	1.35	10.48	206386	1.05
2.290	0.900	240	0.88	12.17	239598	1.22
2.863	1.125	300	0.64	13.72	270059	1.37
$D = 40$ mm						
0.045	0.010	2	1440.9	1.84	36148	0.18
1.357	0.300	60	4.72	4.72	92930	0.47
2.714	0.600	120	1.40	6.44	126757	0.64
4.072	0.900	180	0.76	7.86	154789	0.79
5.429	1.200	240	0.50	9.13	179698	0.91
6.786	1.500	300	0.36	10.29	202544	1.03
$D = 50$ mm						
0.071	0.010	1.6	1392.5	1.42	27947	0.14
2.651	0.375	60	2.63	3.78	74344	0.38
5.301	0.750	120	0.90	5.15	101405	0.52
7.952	1.125	180	0.49	6.29	123831	0.63
10.603	1.500	240	0.32	7.30	143759	0.73
13.254	1.875	300	0.23	8.23	162065	0.82
$D = 60$ mm						
0.107	0.010	1.33	1356.7	1.15	22691	0.12
4.580	0.450	60	1.83	3.15	61954	0.31
9.161	0.900	120	0.62	4.29	84505	0.43
13.741	1.350	180	0.34	5.24	103193	0.52
18.322	1.800	240	0.22	6.08	119799	0.61
22.902	2.250	300	0.16	6.86	135029	0.69

Table 3.5

Values of head loss for paste made from cement CEM II/B-S 32.5 R, $W/C = 0.40$

Q [$m^3 \cdot h^{-1}$]	v [$m \cdot s^{-1}$]	$\dot{\gamma}$ [s^{-1}]	λ [–]	h_{str} [m]	Δp [Pa]	I_m [–]
$D = 20$ mm						
0.078	0.069	38.5	35.52	4.31	82026	0.43
0.170	0.150	60	10.22	5.86	111504	0.59
0.339	0.300	120	3.55	8.14	154899	0.81
0.509	0.450	180	1.96	10.09	192120	1.01
0.679	0.600	240	1.29	11.87	225987	1.19
0.893	0.750	300	0.94	13.54	257619	1.35
$D = 30$ mm						
0.201	0.079	30.4	24.72	2.62	49877	0.26
0.573	0.225	60	4.54	3.91	74336	0.39
1.145	0.450	120	1.58	5.43	103266	0.54
1.718	0.675	180	0.87	6.73	128080	0.67
2.290	0.900	240	0.57	7.92	150658	0.79
2.863	1.125	300	0.42	9.02	171746	0.90
$D = 40$ mm						
0.393	0.087	25.7	19.18	1.85	35205	0.18
1.357	0.300	60	2.55	2.93	55752	0.29
2.714	0.600	120	0.89	4.07	77449	0.41
4.072	0.900	180	0.49	5.05	96060	0.50
5.429	1.200	240	0.32	5.94	112994	0.59
6.786	1.500	300	0.24	6.77	128810	0.68
$D = 50$ mm						
0.664	0.094	22.6	15.72	1.42	26954	0.14
2.651	0.375	60	1.63	2.34	44602	0.23
5.301	0.750	120	0.57	3.26	61959	0.33
7.952	1.125	180	0.31	4.04	76848	0.40
10.603	1.500	240	0.21	4.75	90395	0.47
13.254	1.875	300	0.15	5.41	103048	0.54
$D = 60$ mm						
1.018	0.100	20.3	13.42	1.14	21693	0.11
4.580	0.450	60	1.13	1.95	37168	0.20
9.161	0.900	120	0.39	2.71	51633	0.27
13.741	1.350	180	0.22	3.36	64040	0.34
18.322	1.800	240	0.14	3.96	75329	0.40
22.902	2.250	300	0.10	4.51	85873	0.45

Table 3.6

Values of head loss for paste made from cement CEM II/B-S 32.5 R, W/C = 0.50

Q [$m^3 \cdot h^{-1}$]	v [$m \cdot s^{-1}$]	$\dot{\gamma}$ [s^{-1}]	λ [–]	h_{str} [m]	Δp [Pa]	I_m [–]
D = 20 mm						
0.090	0.080	46.1	14.14	2.31	41169	0.23
0.170	0.150	60	5.14	2.95	52617	0.29
0.339	0.300	120	1.78	4.08	72848	0.41
0.509	0.450	180	0.98	5.07	90500	0.51
0.679	0.600	240	0.65	5.98	106767	0.60
0.893	0.750	300	0.48	6.84	122117	0.68
D = 30 mm						
0.234	0.092	36.6	9.77	1.40	25079	0.14
0.573	0.225	60	2.28	1.96	35078	0.20
1.145	0.450	120	0.79	2.72	48566	0.27
1.718	0.675	180	0.44	3.38	60333	0.34
2.290	0.900	240	0.29	3.99	71178	0.40
2.863	1.125	300	0.21	4.56	81412	0.46
D = 40 mm						
0.457	0.101	31.0	7.62	0.99	17692	0.10
1.357	0.300	60	1.28	1.47	26308	0.15
2.714	0.600	120	0.44	2.04	36424	0.20
4.072	0.900	180	0.25	2.53	45250	0.25
5.429	1.200	240	0.16	2.99	53384	0.30
6.786	1.500	300	0.12	3.42	61059	0.34
D = 50 mm						
0.770	0.109	27.3	6.3	0.76	13551	0.08
2.651	0.375	60	0.82	1.18	21047	0.12
5.301	0.750	120	0.28	1.63	29139	0.16
7.952	1.125	180	0.16	2.03	36200	0.20
10.603	1.500	240	0.10	2.39	42707	0.24
13.254	1.875	300	0.08	2.74	48847	0.27
D = 60 mm						
1.181	0.116	24.6	5.43	0.61	10913	0.06
4.580	0.450	60	0.57	0.98	17539	0.10
9.161	0.900	120	0.20	1.36	24283	0.14
13.741	1.350	180	0.11	1.69	30167	0.17
18.322	1.800	240	0.07	1.99	35589	0.20
22.902	2.250	300	0.05	2.28	40706	0.23

Table 3.7

Values of head loss for paste made from cement CEM II/B-S 32.5 R, $W/C = 0.60$

Q [$m^3 \cdot h^{-1}$]	v [$m \cdot s^{-1}$]	$\dot{\gamma}$ [s^{-1}]	λ [–]	h_{str} [m]	Δp [Pa]	I_m [–]
$D = 20$ mm						
0.113	0.100	57.1	5.51	1.41	23846	0.14
0.170	0.150	60	2.86	1.64	27883	0.16
0.339	0.300	120	0.97	2.23	37860	0.22
0.509	0.450	180	0.53	2.74	46540	0.27
0.679	0.600	240	0.35	3.21	54496	0.32
0.893	0.750	300	0.25	3.65	61976	0.37
$D = 30$ mm						
0.290	0.114	45.0	3.97	0.85	14470	0.09
0.573	0.225	60	1.27	1.09	18548	0.11
1.145	0.450	120	0.43	1.49	25240	0.15
1.718	0.675	180	0.24	1.83	31027	0.18
2.290	0.900	240	0.16	2.14	36331	0.21
2.863	1.125	300	0.11	2.43	41317	0.24
$D = 40$ mm						
0.570	0.126	38.2	2.98	0.60	10225	0.06
1.357	0.300	60	0.71	0.82	13911	0.08
2.714	0.600	120	0.24	1.11	18930	0.11
4.072	0.900	180	0.13	1.37	23270	0.14
5.429	1.200	240	0.09	1.61	27248	0.16
6.786	1.500	300	0.06	1.83	30988	0.18
$D = 50$ mm						
0.961	0.136	33.6	2.45	0.46	7826	0.05
2.651	0.375	60	0.46	0.66	11129	0.07
5.301	0.750	120	0.16	0.89	15144	0.09
7.952	1.125	180	0.09	1.10	18616	0.11
10.603	1.500	240	0.06	1.28	21799	0.13
13.254	1.875	300	0.04	1.46	24790	0.15
$D = 60$ mm						
1.466	0.144	30.2	2.10	0.37	6291	0.04
4.580	0.450	60	0.32	0.55	9274	0.05
9.161	0.900	120	0.11	0.74	12620	0.07
13.741	1.350	180	0.06	0.91	15513	0.09
18.322	1.800	240	0.04	1.07	18165	0.11
22.902	2.250	300	0.03	1.22	20659	0.12

Table 3.8

Values of head loss for paste made from cement CEM II/B-S 32.5 R, W/C = 0.70

Q [$m^3 \cdot h^{-1}$]	v [$m \cdot s^{-1}$]	$\dot{\gamma}$ [s^{-1}]	λ [–]	h_{str} [m]	Δp [Pa]	I_m [–]
D = 20 mm						
0.159	0.141	77.6	1.74	0.88	14326	0.09
0.170	0.150	60	1.57	0.90	14705	0.09
0.339	0.300	120	0.55	1.25	20372	0.13
0.509	0.450	180	0.30	1.56	25381	0.16
0.679	0.600	240	0.20	1.84	30042	0.18
0.893	0.750	300	0.15	2.12	34475	0.21
D = 30 mm						
0.412	0.162	61.7	1.18	0.53	8583	0.05
0.573	0.225	60	0.70	0.60	9830	0.06
1.145	0.450	120	0.24	0.83	13581	0.08
1.718	0.675	180	0.13	1.04	16921	0.10
2.290	0.900	240	0.09	1.23	20028	0.12
2.863	1.125	300	0.07	1.41	22983	0.14
D = 40 mm						
0.805	0.178	35.6	0.91	0.37	5989	0.04
1.357	0.300	60	0.39	0.45	7352	0.05
2.714	0.600	120	0.14	0.63	10186	0.06
4.072	0.900	180	0.08	0.78	12691	0.08
5.429	1.200	240	0.05	0.92	15021	0.09
6.786	1.500	300	0.04	1.06	17328	0.11
D = 50 mm						
1.357	0.192	30.7	0.74	0.28	4550	0.03
2.651	0.375	60	0.25	0.36	5882	0.04
5.301	0.750	120	0.09	0.50	8149	0.05
7.952	1.125	180	0.05	0.62	10152	0.06
10.603	1.500	240	0.03	0.74	12017	0.07
13.254	1.875	300	0.02	0.85	13790	0.08
D = 60 mm						
2.076	0.204	27.2	0.63	0.22	3639	0.02
4.580	0.450	60	0.17	0.30	4901	0.03
9.161	0.900	120	0.06	0.42	6791	0.04
13.741	1.350	180	0.03	0.52	8460	0.05
18.322	1.800	240	0.02	0.61	10014	0.06
22.902	2.250	300	0.02	0.71	11492	0.07

Table 3.9

Values of head loss for paste made with use of cement CEM II/B-S 42.5 N, W/C = 0.40

Q [$m^3 \cdot h^{-1}$]	v [$m \cdot s^{-1}$]	$\dot{\gamma}$ [s^{-1}]	λ [–]	h_{str} [m]	Δp [Pa]	I_m [–]
D = 20 mm						
0.079	0.070	28	68.05	8.50	161731	0.85
0.170	0.150	60	19.28	11.05	210352	1.11
0.339	0.300	120	6.65	15.25	290209	1.52
0.509	0.450	180	3.59	18.55	353068	1.86
0.679	0.600	240	2.33	21.38	406964	2.14
0.893	0.750	300	1.67	23.91	455055	2.39
D = 30 mm						
0.204	0.080	21.3	47.28	5.14	97849	0.51
0.573	0.225	60	8.57	7.37	140235	0.74
1.145	0.450	120	2.95	10.17	193472	1.02
1.718	0.675	180	1.60	12.37	235379	1.24
2.290	0.900	240	1.04	14.26	271310	1.43
2.863	1.125	300	0.74	15.94	303370	1.59
D = 40 mm						
0.398	0.088	17.6	36.60	3.61	68738	0.36
1.357	0.300	60	4.82	5.53	105176	0.55
2.714	0.600	120	1.66	7.62	145104	0.76
4.072	0.900	180	0.90	9.28	176534	0.93
5.429	1.200	240	0.58	10.69	203482	1.07
6.786	1.500	300	0.42	11.96	227528	1.20
D = 50 mm						
0.664	0.094	15	30.47	2.74	52231	0.27
2.651	0.375	60	3.08	4.42	84141	0.44
5.301	0.750	120	1.06	6.10	116083	0.61
7.952	1.125	180	0.58	7.42	141227	0.74
10.603	1.500	240	0.37	8.55	162786	0.86
13.254	1.875	300	0.27	9.56	182022	0.96
D = 60 mm						
1.018	0.100	13.3	25.91	2.20	41893	0.22
4.580	0.450	60	2.14	3.68	70117	0.37
9.161	0.900	120	0.74	5.08	96736	0.51
13.741	1.350	180	0.40	6.18	117689	0.62
18.322	1.800	240	0.28	7.13	135655	0.71
22.902	2.250	300	0.18	7.97	151685	0.80

Table 3.10

Values of head loss for paste made from cement CEM II/B-S 42.5 N, $W/C = 0.50$

Q [$m^3 \cdot h^{-1}$]	v [$m \cdot s^{-1}$]	$\dot{\gamma}$ [s^{-1}]	λ [–]	h_{str} [m]	Δp [Pa]	I_m [–]
$D = 20$ mm						
0.081	0.072	28.8	33.93	4.48	80027	0.45
0.170	0.150	60	10.48	6.01	107309	0.60
0.339	0.300	120	3.63	8.32	148574	0.83
0.509	0.450	180	1.99	10.28	183457	1.03
0.679	0.600	240	1.31	12.03	214873	1.20
0.893	0.750	300	0.95	13.67	243982	1.37
$D = 30$ mm						
0.209	0.082	21.9	23.75	2.71	48447	0.27
0.573	0.225	60	4.66	4.01	71539	0.40
1.145	0.450	120	1.61	5.55	99049	0.55
1.718	0.675	180	0.88	6.85	122305	0.69
2.290	0.900	240	0.58	8.02	143249	0.80
2.863	1.125	300	0.42	9.11	162654	0.91
$D = 40$ mm						
0.412	0.091	18.2	18.16	1.92	34207	0.19
1.357	0.300	60	2.62	3.00	53654	0.30
2.714	0.600	120	0.91	4.16	74287	0.42
4.072	0.900	180	0.50	5.14	91729	0.51
5.429	1.200	240	0.33	6.02	107437	0.60
6.786	1.500	300	0.24	6.83	121991	0.68
$D = 50$ mm						
0.693	0.098	15.7	14.94	1.46	26118	0.15
2.651	0.375	60	1.68	2.40	42924	0.24
5.301	0.750	120	0.58	3.33	59430	0.33
7.952	1.125	180	0.32	4.11	73383	0.41
10.603	1.500	240	0.21	4.81	85949	0.48
13.254	1.875	300	0.15	5.47	97593	0.55
$D = 60$ mm						
1.059	0.104	13.9	12.79	1.17	20975	0.12
4.580	0.450	60	1.16	2.00	35770	0.20
9.161	0.900	120	0.40	2.77	49525	0.28
13.741	1.350	180	0.22	3.42	61153	0.34
18.322	1.800	240	0.15	4.01	71624	0.40
22.902	2.250	300	0.11	4.56	81327	0.46

Table 3.11

Values of head loss for paste made from cement CEM II/B-S 42.5 N, $W/C = 0.60$

Q [$m^3 \cdot h^{-1}$]	v [$m \cdot s^{-1}$]	$\dot{\gamma}$ [s^{-1}]	λ [–]	h_{str} [m]	Δp [Pa]	I_m [–]
$D = 20$ mm						
0.100	0.088	35.2	10.46	2.06	35034	0.21
0.170	0.150	60	4.38	2.51	42664	0.25
0.339	0.300	120	1.48	3.40	57732	0.34
0.509	0.450	180	0.81	4.16	70605	0.42
0.679	0.600	240	0.53	4.85	82303	0.49
0.893	0.750	300	0.38	5.49	93226	0.55
$D = 30$ mm						
0.254	0.100	26.7	7.40	1.26	21326	0.13
0.573	0.225	60	1.95	1.68	28443	0.17
1.145	0.450	120	0.66	2.27	38488	0.23
1.718	0.675	180	0.36	2.72	47070	0.28
2.290	0.900	240	0.23	3.23	54869	0.32
2.863	1.125	300	0.17	3.66	62151	0.37
$D = 40$ mm						
0.498	0.110	22	5.77	0.89	15087	0.09
1.357	0.300	60	1.10	1.26	21332	0.13
2.714	0.600	120	0.37	1.70	28866	0.17
4.072	0.900	180	0.20	2.08	35303	0.21
5.429	1.200	240	0.13	2.42	41152	0.24
6.786	1.500	300	0.10	2.75	46613	0.27
$D = 50$ mm						
0.841	0.119	19	4.73	0.68	11577	0.07
2.651	0.375	60	0.70	1.01	17066	0.10
5.301	0.750	120	0.24	1.36	23093	0.14
7.952	1.125	180	0.13	1.66	28242	0.17
10.603	1.500	240	0.08	1.94	32921	0.19
13.254	1.875	300	0.06	2.20	37291	0.22
$D = 60$ mm						
1.283	0.126	16.8	4.03	0.55	9320	0.05
4.580	0.450	60	0.65	0.78	13249	0.08
9.161	0.900	120	0.22	1.04	17682	0.10
13.741	1.350	180	0.12	1.26	21451	0.13
18.322	1.800	240	0.08	1.47	24870	0.15
22.902	2.250	300	0.06	1.65	28057	0.17

Table 3.12

Values of head loss for paste made from cement CEM II/B-S 42.5 N, $W/C = 0.70$

Q [$m^3 \cdot h^{-1}$]	v [$m \cdot s^{-1}$]	$\dot{\gamma}$ [s^{-1}]	λ [–]	h_{str} [m]	Δp [Pa]	I_m [–]
$D = 20$ mm						
0.130	0.115	46	4.79	1.61	26287	0.16
0.170	0.150	60	3.12	1.79	29173	0.18
0.339	0.300	120	1.06	2.43	39516	0.24
0.509	0.450	180	0.57	2.96	48175	0.30
0.679	0.600	240	0.37	3.43	55928	0.34
0.893	0.750	300	0.27	3.87	63083	0.39
$D = 30$ mm						
0.336	0.132	35.2	3.30	0.98	15887	0.10
0.573	0.225	60	1.39	1.19	19449	0.12
1.145	0.450	120	0.47	1.62	26344	0.16
1.718	0.675	180	0.25	1.97	32116	0.20
2.290	0.900	240	0.17	2.29	37285	0.23
2.863	1.125	300	0.12	2.58	42055	0.26
$D = 40$ mm						
0.656	0.145	29	2.55	0.68	11145	0.07
1.357	0.300	60	0.78	0.90	14587	0.09
2.714	0.600	120	0.26	1.21	19758	0.12
4.072	0.900	180	0.14	1.48	24087	0.15
5.429	1.200	240	0.09	1.71	27964	0.17
6.786	1.500	300	0.07	1.94	31541	0.19
$D = 50$ mm						
1.103	0.156	25	2.10	0.52	8486	0.05
2.651	0.375	60	0.50	0.72	11669	0.07
5.301	0.750	120	0.17	0.97	15806	0.10
7.952	1.125	180	0.09	1.18	19270	0.12
10.603	1.500	240	0.06	1.37	22371	0.14
13.254	1.875	300	0.04	1.55	25233	0.15
$D = 60$ mm						
1.690	0.166	22.1	1.79	0.42	6808	0.04
4.580	0.450	60	0.35	0.60	9724	0.06
9.161	0.900	120	0.12	0.81	13172	0.08
13.741	1.350	180	0.06	0.99	16058	0.10
18.322	1.800	240	0.04	1.14	18643	0.11
22.902	2.250	300	0.03	1.29	21028	0.13

3.6. The determination of head loss in horizontal pipelines

The description of rheological properties of cement pastes by means of the determination of their rheological parameters enables to generalize the test results by the application of the non-dimensional criterion $\lambda(Re_{gen})$, linking the non-dimensional Darcy friction factor λ of the pipe with the generalized Reynolds number $Re_{H,gen}$.

Total head loss on the pipe length L can be calculated with use of the classic Darcy–Weisbach equation:

$$h_{str} = \lambda \frac{L}{D} \frac{v^2}{2g} \tag{3.19}$$

This equation is often transformed to such form that allows the determination of the pressure loss on the pipe length L:

$$\Delta p = \lambda \frac{L}{D} \frac{v^2}{2} \rho \tag{3.20}$$

Or the decrease of energy line

$$I_m = \lambda \frac{1}{D} \frac{v^2}{2g} \tag{3.21}$$

Knowledge of the rheological parameters of cement pastes and the lengths of the planned pipelines enables us to calculate the head loss for the adopted diameters D and volumetric flow rates Q.

Sample values of the calculations conducted for a pipe of the length L of 10 m and diameter D varying within the range from 20 to 60 mm are listed in Tables 3.4–3.12 and presented in graphic form in Figures 3.14–3.22, in form of a function $h_{str}(v)$.

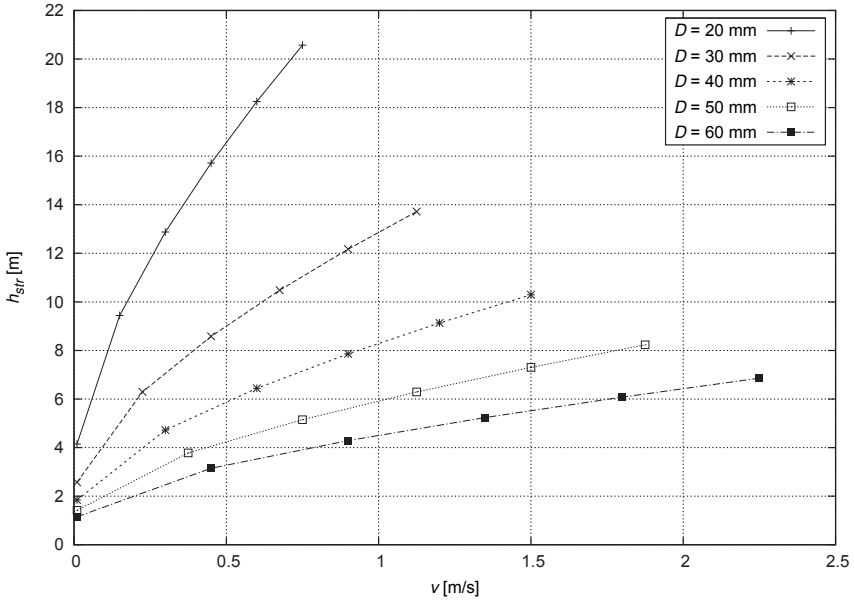

Fig. 3.14. Relation between the head loss h_{str} and the flow rate v for different pipe diameters D. Paste made from cement CEM II/B-S 32.5 R, W/C = 0.35

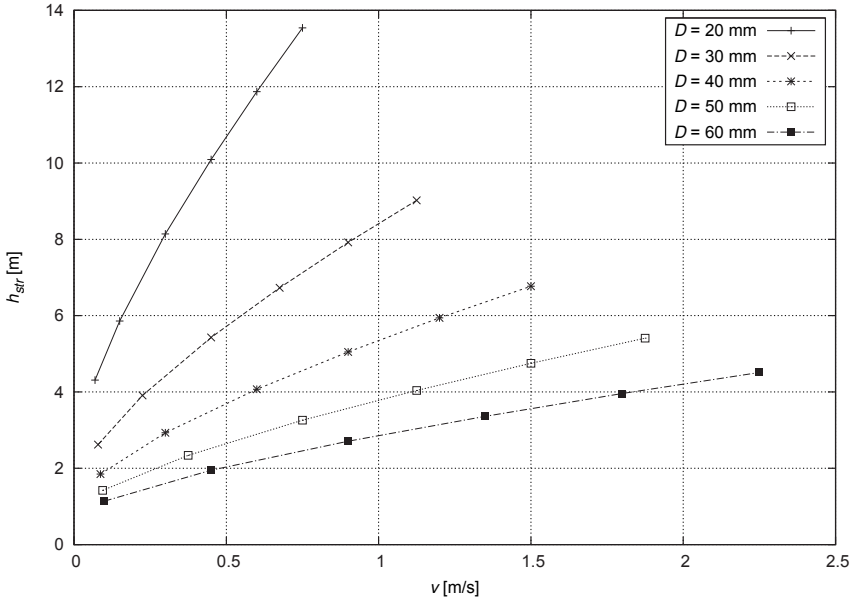

Fig. 3.15. Relation between the head loss h_{str} and the flow rate v for different pipe diameters D. Paste made from cement CEM II/B-S 32.5 R, W/C = 0.40

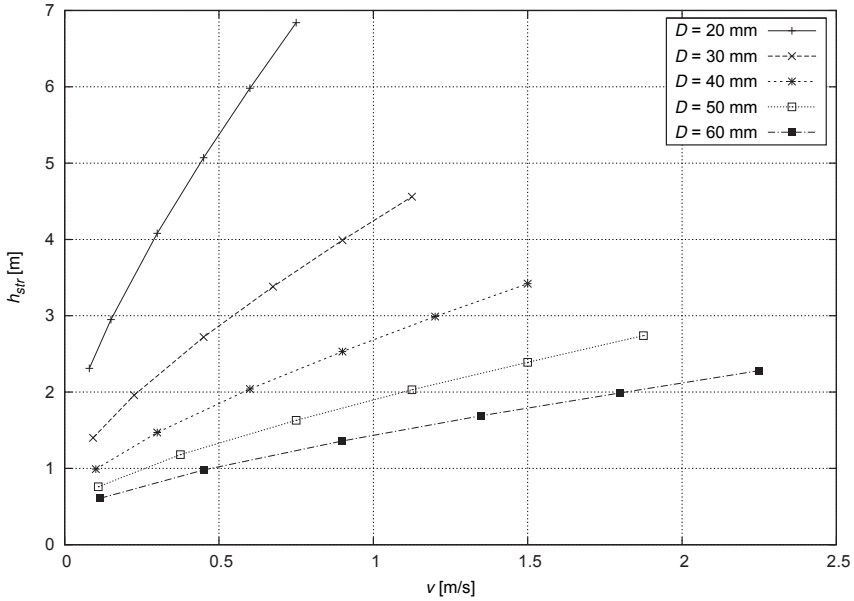

Fig. 3.16. Relation between the head loss h_{str} and the flow rate v for different pipe diameters D. Paste made from cement CEM II/B-S 32.5 R, W/C = 0.50

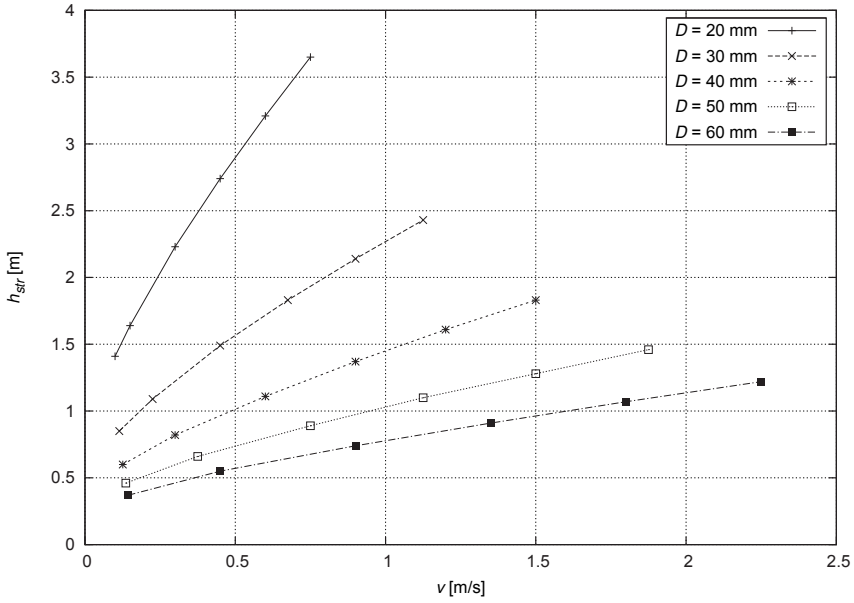

Fig. 3.17. Relation between the head loss h_{str} and the flow rate v for different pipe diameters D. Paste made from cement CEM II/B-S 32.5 R, W/C = 0.60

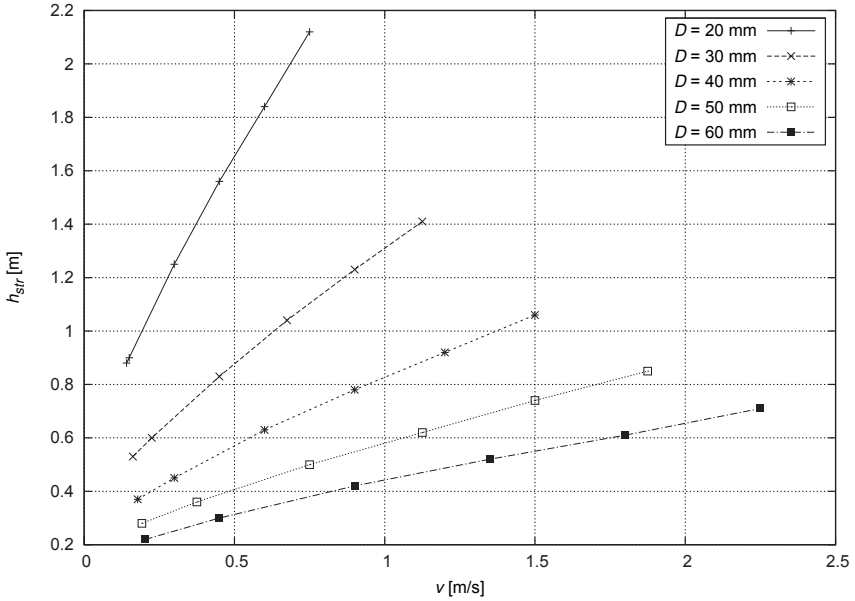

Fig. 3.18. Relation between the head loss h_{str} and the flow rate v for different pipe diameters D. Paste made from cement CEM II/B-S 32.5 R, W/C = 0.70

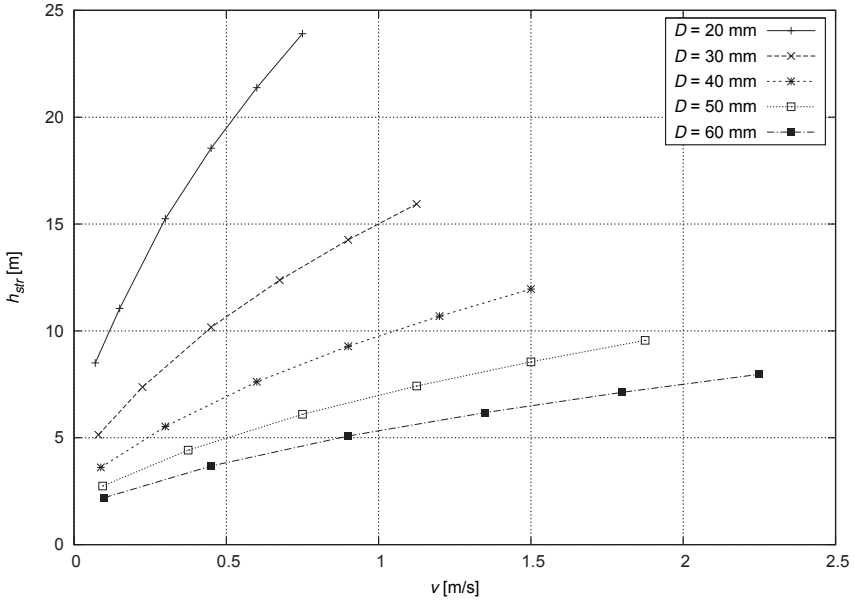

Fig. 3.19. Relation between the head loss h_{str} and the flow rate v for different pipe diameters D. Paste made from cement CEM II/B-S 42.5 N, W/C = 0.40

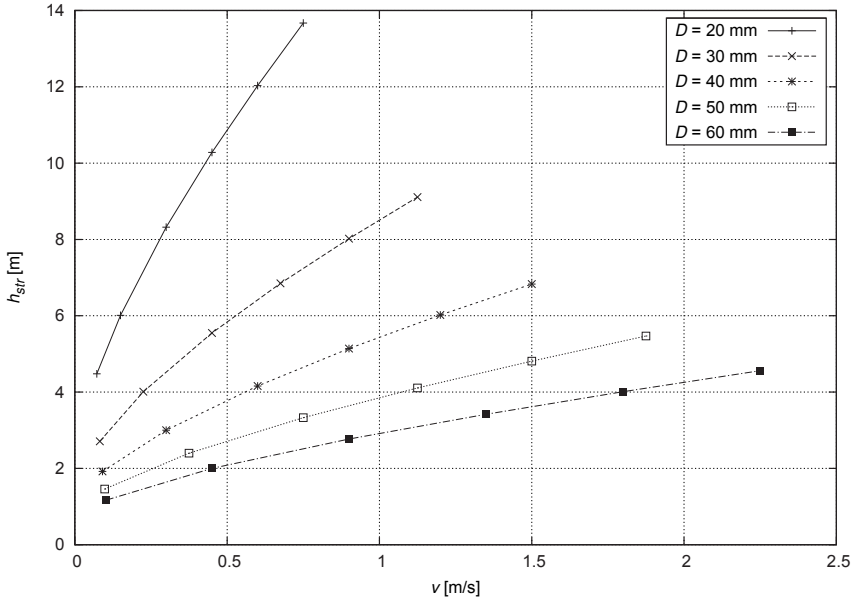

Fig. 3.20. Relation between the head loss h_{str} and the flow rate v for different pipe diameters D. Paste made from cement CEM II/B-S 42.5 N, W/C = 0.50

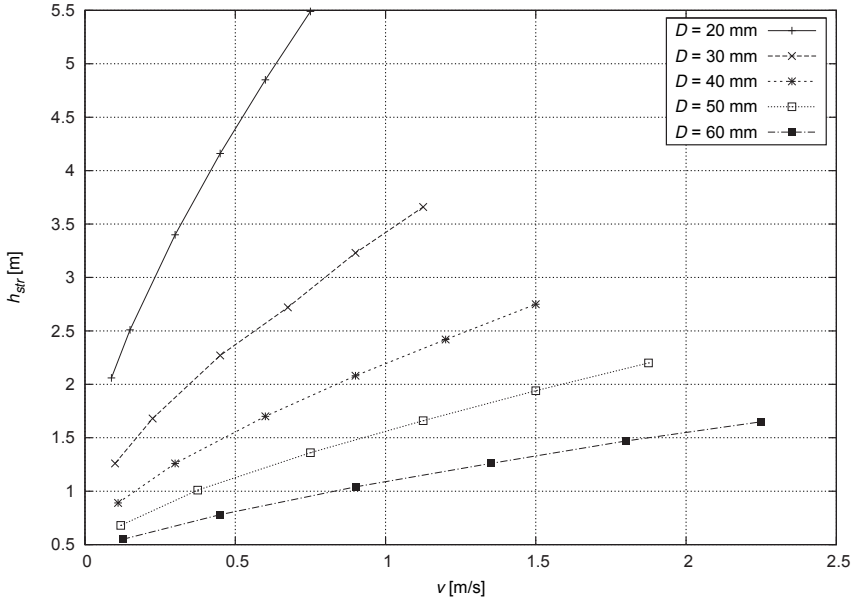

Fig. 3.21. Relation between the head loss h_{str} and the flow rate v for different pipe diameters D. Paste made from cement CEM II/B-S 42.5 N, W/C = 0.60

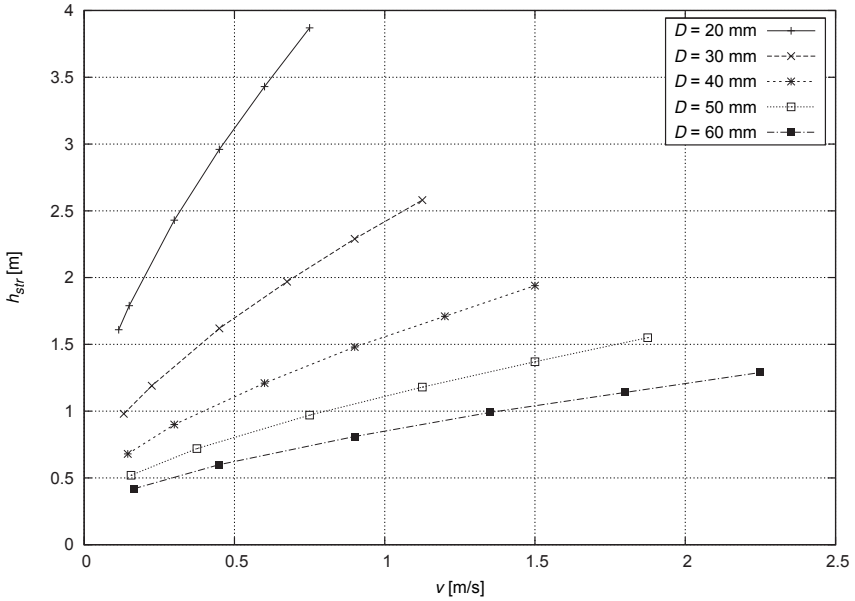

Fig. 3.22. Relation between the head loss h_{str} and the flow rate v for different pipe diameters D. Paste made from cement CEM II/B-S 42.5 N, W/C = 0.70

4. CO-OPERATION OF THE PUMPING ENGINE WITH THE PRESSURE PIPE

The choice of pumping engine for the designed installation for the hydraulic transport of cement pastes is based on the analysis of the so-called working point of the pump with the pressure pipe. This point lies at the crossing of the characteristics of the pump $H = f(Q)$ and the curve describing total decrease of energy in the pressure pipe $H_c = f(Q)$.

The hydraulic characteristics of the pressure pump $H = f(Q)$ is received from the manufacturer, as the basic parameter describing the scope of its practical application. In the majority of cases of pipe transport of cement pastes and derived materials, piston pumps are used. The characteristic of such pump is a straight line parallel to axis H, at the constant value of volumetric flow rate Q.

The total loss of energy H_c is determined according to the following formula:

$$H_c = h_{str} + \frac{\alpha_s v^2}{2g} + \frac{p_k}{\rho g} + H_{geo} \tag{4.1}$$

This formula can be transformed to a formula describing total pressure loss:

$$\Delta p_c = \Delta p + \frac{\alpha_s v^2}{2}\rho + p_k + H_{geo}\rho g \tag{4.2}$$

The value of head loss h_{str} or pressure loss Δp is calculated with use of the Darcy–Weisbach equation (3.19), (3.20). The pipe length assumed for the purpose of these equations in increased by an equivalent length L^*, illustrating local pressure loss related to the embedded fittings (valves, elbows, turns etc.)

$$L^* = \xi \frac{D}{\lambda} \tag{4.3}$$

where ξ is the minor loss coefficient for various types of fittings. The application of the formula (4.3) and the calculation of the substitute length L^* allow to take into account the rheological properties of cement pastes for different concentrations of the mixture.

The value of the expression $\alpha_s v^2/2g$, enabling the determination of the so-called velocity height, is practically insignificant. For pipe transport of cement pastes characterized by a high concentration of solid particles, in laminar flow (at low rates of flow), such assumption is, in our opinion completely justified. In the case of hydraulic transport at high volumetric flow rate, and corresponding high velocity of flow, the value of this expression becomes significant (Saint-Venant's coefficient for turbulent flow $\alpha_s \approx 1$ [16]).

The parameter p_k describes the so-called working pressure on the outlet of the pipe, and is closely related to the applied technology of use of hydraulic transport. In the case of injection installations the recommended working pressure should fall into the range between 0.2–1.0 MPa [19].

The determination of the characteristics $p_c = f(Q)$ for various diameters of the pressure pipe D and various mass concentrations C_s (various values of the water to cement ratio W/C) and the pump characteristics describing the relation between the forcing pressure p and the volumetric flow rate Q, $p = f(Q)$ allows to determine the working point of the analysed pump-pipe system.

Sample determination of the working point for the flow of cement paste made from cement CEM II/B-S 32.5 R in a horizontal pressure pipe ($H_{geo} = 0$) of the diameter $D = 50$ mm and length $L = 10$ m and working pressure $p_k = 0.4$ MPa, co-operating with a constant capacity piston pump $Q = 75$ dm^3/min, is presented in Figures 4.1 and 4.2.

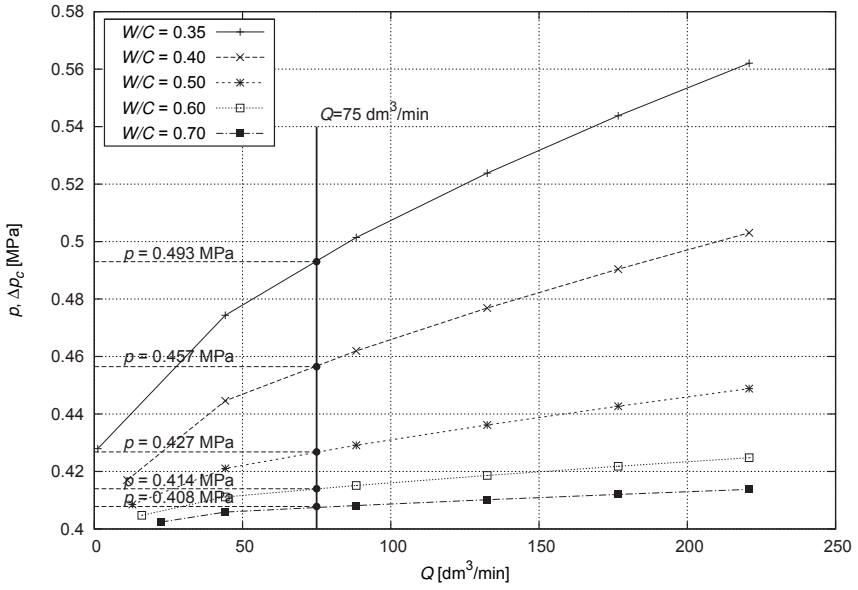

Fig. 4.1. Sample determination of the working point for a horizontal pipe of the diameter $D = 50$ mm, transporting cement pastes made from cement CEM II/B-S 32.5 R of various concentrations

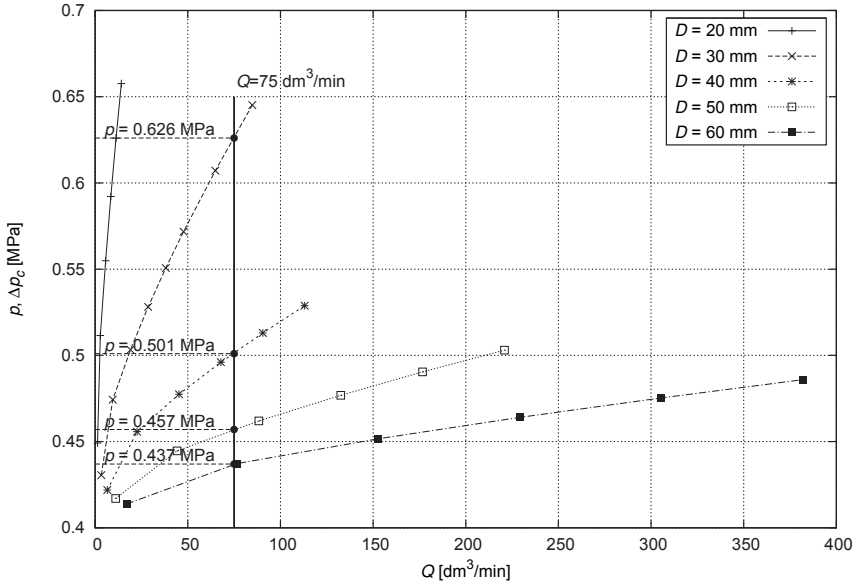

Fig. 4.2. Sample determination of the working point for a horizontal pipe of various diameters *D*, transporting cement pastes made from cement CEM II/B-S 32.5 R, at water to cement ratio *W/C* = 0.40

Figure 4.2 enables us to determine the range of variability of the pressure that is necessary for the pressing of a constant volumetric flow (Q = 75 dm^3/min) of cement pastes of a given concentration (*W/C* = 0.40), for different pressure pipe diameters *D*. The pressure p in this case varies within the range from 0.437 to 0.626 MPa. For the diameter D = 20 mm, the working point of the pump-pipe system cannot be determined on the graph.

The analysis of the above diagrams allows to conduct a further, economic analysis of the designed installation for hydraulic transport, and to decide, whether it would be better to assume a larger pipe diameter for lower pressures of flow, or to design a smaller diameter and allow for higher pressure of flow in the pipe.

Thus, working points enable to determine the optimal forcing pressure in order to ensure the proper regimen of operation of the installation and the correct measurement of the pressing pipe in the terms of the strength of materials (choice of suitable materials for the construction of the pipe).

The analysis of the co-operation allows, eventually, to determine the optimal pipe diameter D and concentration *Cs* (water to cement ratio *W/C*) of the pressed mixture, for the planned pumping engine.

5. CONCLUSION

This monograph presents a comprehensive solution of the problems related to the use of pipe transport of liquid cement pastes and derivative materials for various technological installations for their practical application.

In this case, the development has to be preceded by laboratory tests of the physical, rheological and sedimentation properties of the transported mixture. This will allow to conduct the procedures suggested here, which enable the determination of parameters necessary in order to ensure the optimal functioning of the hydraulic transport installation.

The determination of the physical properties of a mixture consists in standard tests that enable the determination of solid particles density, density of the mixture, granulation characteristics, specific surface area, mass or volume concentration, water to cement ratio, binding time characteristics, etc.

On the other hand, rheological tests allow to prepare a detailed rheological characteristic of the mixture, which constitutes a basis for further analyses and calculations that enable the determination of the hydraulic parameters of the flow of cement pastes in pipes. These tests are conducted with use of rotational viscometers that do not require costly pipe installations, and are possible to conduct in a short time. However, one should bear in mind, that liquid cement pastes are non-Newtonian liquids, and that rheological tests should be conducted in compliance with the principle of maintaining the rheological stability of the tested material [16]. The apparent curves of flow obtained as a result of the measurements are then transposed into actual curves of flow, thus allowing to choose the correct rheological model through statistical analysis and the resulting determination of the required rheological parameters of the adopted model. The plastic-viscous nature of behaviour of cement pastes requires the application of tri-parametric, general rheological models. The Herschel–Bulkley model has proved to be optimal for this purpose. This model features a characteristic yield stress τ_0, and after it is exceeded, flow occurs in the pipe.

Rheological parameters allow to further determine the characteristic hydraulic values of the mixture. One of these is the general Reynolds number for the adopted model. It allows to classify the regimen of flow of the mixture in the pipe. Critical Reynolds number differentiates between laminar and turbulent flow of the mixture. Hence, it is a crucial parameter, considering that hydraulic transport of highly concentrated cement pastes takes place in the laminar regimen of flow. Thus, the range of acceptable velocities of flow should be calculated. The flow should take place at the average velocity $v_{sr,}$

in the range between transient velocity v_{gr} and critical velocity v_{kr}. The critical velocity corresponds to the flow described by critical Reynolds number Re_{kr}, whereas transient velocity separates the regimens of homogeneous and heterogeneous mixtures with movable bottom, which are determined basing on sedimentation tests, conducted in cylindrical sedimentation columns. They allow to calculate the fall velocity of solid particles, which eventually makes it possible to calculate transient velocity v_{gr} according to Newitt. This velocity can be also determined with use of the Durand formula. The authors have assumed for the tested cements the values of the non-dimensional coefficient F_L that may fall within the range $F_L = 0.1 - 0.3$.

After the determination of the ultimate range of velocities for laminar flow, pressure loss is determined for the flow of the mixture at various pipe diameters D and various concentrations C_s (water to cement ratio W/C). These calculations are performed basing on the non-dimensional criterion λ (Re_{gen}), determining the relation between the obtained Darcy friction factor λ and the general Reynolds number Re_{gen}, describing the rheological properties of the transported medium.

Knowing the characteristics of pressure loss in pipe and the characteristics of the applied pumping engine, the working point of the pump-pipe system of the developed installation is determined. This enables a complete analysis of the range of occurring pressures and the realisation of the design of the pipe in the terms of construction and material strength.

The realization of the above specified procedures fulfils the objectives of this monograph.

The conducted tests can constitute a basis for important conclusions in the field of practical engineering:

1. Cement pastes, at such concentrations C_s ($W/C \leq 0.7$) that are usually applied in practice, behave like non-Newtonian liquids of a viscoplastic nature, with a variable plastic viscosity η_{pl}. The approximation of flow curves requires a general, tri-parametric rheological model.
2. The recommended rheological model is the general, tri-parametric Herschel–Bulkley model which can be transformed into simpler, bi-parametric and single-parameter models, in the conditions of simplification of the internal structure of cement pastes.
3. Rheological tests should be conducted with use of a rotational viscometer, with the possibility to determine the characteristic yield stress τ_0, for a wide range of concentrations C_s, or water to cement ratios W/C. This will allow to determine the transient concentration, differentiating between Newtonian and non-Newtonian behaviour of the mixture, and to present the relation between rheological parameters as a function of concentration: τ_0 (C_s), k(C_s), n(C_s).
4. The test results should be generalised basing on the non-dimensional criterion λ(Re_{gen}), linking the Darcy friction factor λ with the general Reynolds number Re_{gen}, taking into account the rheological properties of cement pastes.

BIBLIOGRAPHY

[1] Ancey C., 2005. Solving the Couette inverse problem using a wavelet-vaguelette decomposition. Journal of Rheology, 49(2): 441–460.

[2] Atzeni C., Massida C., Sanna U., 1985. Comparison between rheological models for portland cement pastes. Cement and Concrete Research, 15: 511–519.

[3] Banfill P.F.G., 2003. The rheology of fresh cement and concrete – a review. Proceedings of the 11th International Congress on the Chemistry of Cement, Durban, South Africa, wolumen 1, 50–62.

[4] Barnes H.A., 2000. A Handbook of Elementary Rheology. University of Wales Institute of Non-Newtonian liquid Mechanics.

[5] Czaban S., 1987. Wyznaczanie parametrów hydrotransportu rurowego reostabilnych mieszanin dwufazowych. Zeszyty Naukowe Akademii Rolniczej we Wrocławiu, 60, Wydawnictwo Akademii Rolniczej we Wrocławiu, Wrocław.

[6] D'Aloia Schwartzentruber L., Le Roy R., Cordin J., 2006. Rheological behaviour of fresh cement pastes formulated from a self compacting concrete (scc). Cement and Concrete Research, 36: 1203–1213.

[7] Dymaczewski Z., Jeż-Walkowiak J., Marlewski A., Sozański M., 2008. Podstawy reologii i transportu rurowego zawiesin i osadów z oczyszczania wody i ścieków. Monografie 53. Komitet Inżynierii Środowiska PAN Poznań.

[8] Eckstadt H., Hummel H.G., 1977. Ermittlung der kritischen Ablagerngsgeschwindigkeit beim Transport von Gülle in Druckrohrleitungen. W.P. Universität Rostock.

[9] Ferguson J., Kembłowski Z., 1995. Reologia stosowana płynów. Wydawnictwo MAR-CUS sc, Łódź.

[10] Ferraris C.F., 1999. Measurement of the rheological properties of cement paste: a new approach. RILEM International Symposium Proceedings, wolumen 5: 333–341.

[11] Grzeszczyk S., Kucharska L., 1991. The influence of chemical composition of cement on the rheological properties. BANFILL P.F.G., redaktor, Rheology fo Fresh Cement and Concrete, 27–36, Spon.

[12] Jamroży Z., 2009. Beton i jego technologie. Nowe wydanie uwzględniające normę PN EN 206-1. PWN.

[13] Jones T.E.R., Taylor S., 1977. A mathematical model for the low curve of cement paste. Magazine of Concrete Research, 29: 207–212.

[14] Kelessidis V., Maglione R., 2008. Shear rate corrections for Herschel–Bulkley fluids in couette geometry. Applied Rheology, 18: 34482–1–34482–11.
[15] Kelessidis V.C., Maglione R., 2006. Modeling rheological behavior of bentonite su-spensions as Casson and Robertosn–Stiff fluids using Newtonian and true shear rates in Couette viscometry. Powder Technology, 168: 134–147.
[16] Kempiński J., 2000. Hydrauliczna i reologiczna charakterystyka gnojowicy utylizowanej w rolnictwie, wolumen Rozprawy CLXIX serii Zeszyty Naukowe Akademii Rolniczej we Wrocławiu. Wydawnictwo Akademii Rolniczej we Wrocławiu, Wrocław.
[17] Kempiński J., 2001. Flow characteristic of homogenous mixture in laminar flow zone. Archives of Hydro-Engineering and Environmental Mechanics, 48(4): 57–68.
[18] Kilian W., 2008. Ocena wpływu temperatury, czasu i koncentracji na cechy reologiczne płynnych zaczynów cementowych. Wydawnictwo Uniwersytetu Przyrodniczego we Wrocławiu, Wrocław.
[19] Król M., Szerafin J., 2001. Reologia w procsie iniekcji zaczynami cementowymi. III Sympozjum Naukowo-Techniczne Reologia w technologii betonu: 25–36. Gliwice.
[20] Lapasin R., Papo A., Rajgelj S., 1983. The phenomenological description of the thixo-tropic behaviour of fresh cement pastes. Rheologica Acta, 22: 410–416.
[21] Nehdi M., Rahman M.A., 2004. Estimating rheological properties of cement pastes using various rheological models for different test geometry, gap and surface friction. Cement and Concrete Research, 34: 1993–2007.
[22] Papo A., 1988. Rheological models of cement pastes. Materials and Structures, (21): 41–46.
[23] Parzonka W., 1977. Hydrauliczne podstawy transportu rurowego mieszanin dwufazowych. Wydawnictwo uczelniane Akademii Rolniczej we Wrocławiu, Wrocław.
[24] Rahman M.A., Nehdi M., 2003. Effect of geometry, gap and surface friction of test accessory on measured rheological properties of cement paste. ACI Material Journal, 100(4): 331–339.
[25] Rudziński L., 1983. Reologia świeżych zaczynów cementowych. Budownictwo, 16. Zeszyty Naukowe Politechniki Świętokrzyskiej.
[26] Ryan N.W., Johnson M.W., 1959. Transition from laminar to turbulent flow in pipes. AIChE Journal, 5.
[27] Shou-Chang D., Xue-Bing Z., Ying-Hui Q., Guan-Xiang L., 2007. Rheological characteristic of cement clean paste and folowing behaviour of fresh mixing concrete with pumping in pipeline. J. Cent. Univ. Technol., 14: 462–465.
[28] Szwabowski J., 1987. Urabialność mieszanki betonowej w ujęciu reologicznym. Numer 65 serii Budownictwo. Zeszyty Naukowe Politechniki Śląskiej.
[29] Szwabowski J., 2009. Reologia w technologii betonów. Wydawnictwo Politechniki Śląskiej.
[30] Tattersall G.H., Banfill P.F.G., 1983. The Rheology of Fresh Concrete. Pitman Advanced Pub. Program, London.

[31] Troskolański A.W., 1967. Hydromechanika. WNT.
[32] Vom Berg W., 1979. Influence of specific surface and concentration of solids upon the flow behaviour of cement pastes. Magazine of Concrete Research, 31: 211.
[33] Williams D.A., Saak A.W., Jennings H.M., 1999. The influence of mixing on the rheology of fresh cement pastes. Cement and Concrete Research, 29: 1491–1496.
[34] Yahia A., Khayat K.H., 2003. Aplicability of rheological models to high–performance grouts containing supplementary cementitious materials and viscosity enhancing admixture. Materials and Structures, 36: 402–412.

Rheological foundations of the hydraulic transport of cement pastes

Abstract

This study presents the rheological tests of cement pastes of various mass concentrations C_s, corresponding to various water to cement ratios *W/C*. The tests were conducted with use of Couette-Sarle rotational viscometer, for cement pastes prepared with use of two types of cement: CEM II/B-S 32.5 R i CEM II/B-S 42.5 N, at concentrations corresponding to water to cement ratio *W/C* fluctuating within the range from 0.35 to 0.70.

The curves of flow were approximated with use of the tri-parametric, general rheological Herschel–Bulkley model. This model provides an optimal description of rheological properties of cement pastes that behave like viscoplastic mixtures, with a characteristic yield stress τ_0. The conducted tests allow us to generalize the obtained results with use of the non-dimensional criterion $\lambda(Re_{gen})$, linking the Darcy friction factor λ of the pipe to the general Reynolds number Re_{gen}, describing the rheological properties of cement pastes.

This constitutes a basis for the determination and analysis of the operation of pump-pipe systems used for the transportation of cement pastes for different application technologies, in the laminar zone of flow.

Key words: cement pastes, rheological models, Reynolds number, laminar flow, head loss, pump-pipe transport

Reologiczne podstawy hydrotransportu zaczynów cementowych

Streszczenie

W pracy przedstawiono badania reologiczne zaczynów cementowych o różnych koncentracjach wagowych C_s, odpowiadających różnym wskaźnikom wodno-cementowym *W/C*. Badania przeprowadzono za pomocą wiskozymetru rotacyjnego typu Couette'a-Sarle'a, dla zaczynów cementowych wykonywanych przy użyciu dwóch cementów: CEM II/B-S 32.5 R i CEM II/B-S 42.5 N, przy koncentracjach odpowiadających wskaźnikowi wodno-cementowemu *W/C* zmieniającemu się w przedziale od 0.35 do 0.70.

Aproksymację krzywych płynięcia przeprowadzono za pomocą trójparametrowego, uogólnionego modelu reologicznego Herschela–Bulkley'a. Model ten optymalnie opisuje cechy reologiczne zaczynów cementowych, zachowujących się jak mieszaniny plastyczno-lepkie, z charakterystycznym progiem płynięcia τ_0. Przeprowadzone badania pozwalają na uogólnienie uzyskanych wyników za pomocą bezwymiarowego kryterium $\lambda(Re_{gen})$, wiążącego współczynniki oporu rurociągu λ, z uogólnioną liczbą Reynoldsa Re_{gen}, ujmującą cechy reologiczne zaczynów cementowych.

Stanowi to podstawę do określenia i analizy pracy instalacji pompowo-rurowych, stosowanych do transportowania zaczynów cementowych przy różnych technologiach ich wykorzystywania, w laminarnej strefie przepływu.

Słowa kluczowe: zaczyny cementowe, modele reologiczne, liczba Reynoldsa, ruch laminarny, straty hydrauliczne, transport pompowo-rurowy